

BEACON: Bayesian Optimal Stopping for Efficient LLM Sampling

Anonymous ACL submission

Abstract

Sampling multiple responses is a common way to improve LLM output quality, but it comes at the cost of additional computation. The key challenge is deciding when to stop generating new samples to balance accuracy gains against efficiency. To address this, we introduce BEACON (Bayesian Efficient Adaptive Criterion for Optimal N-stopping), a principled adaptive sampling framework grounded in Sequential Search with Bayesian Learning. BEACON sequentially generates responses from the policy LLM, updates posterior belief over reward distributions in real time without further training, and determines when to stop by weighing expected gains against computational cost. Sampling terminates once the marginal utility of further exploration no longer justifies the expense. We establish both theoretical optimality guarantees and practical tractability, and show empirically that BEACON reduces average sampling by up to 80% while maintaining response quality. We further demonstrate BEACON’s utility for cost-efficient preference data generation and outline practical extensions, offering actionable insights for future researchers.

1 Introduction

Large Language Models (LLMs) have shown human-like abilities across diverse tasks such as mathematics, coding, and creative writing (Ke et al., 2025; Hendrycks et al., 2021). Yet, they often produce inconsistent outputs, occasionally hallucinated on queries they could solve correctly across different runs (Manakul et al., 2023; Xu et al., 2025). To address this, **sampling** has been widely adopted: by generating multiple responses and selecting one based on specific criteria, it improves performance in tasks like complex reasoning (Wang et al., 2022; Snell et al., 2025), safety alignment (Ichihara et al., 2025), and preference data generation (Yuan et al., 2024). However, blindly scaling computational resources is subop-

timal and impractical, particularly in settings such as streaming or real-time LLM applications (Xiao et al., 2024), where efficiency is as critical as **response quality** (Yehudai et al., 2025). This highlights the need for a deeper understanding of the **economy of inference**—balancing computational cost against performance gains.

Existing adaptive sampling methods are mainly based on sample-consistency heuristics to estimate task difficulty or confidence (Aggarwal et al., 2023; Wang et al., 2022; Wan et al., 2025b; Taubenfeld et al., 2025; Wan et al., 2025a). While training-free and easy to implement, these approaches often fail to generalize (Fu et al., 2024; Wang et al., 2025a) because multiple incorrect responses can exhibit consistency, and measuring consistency remains challenging for **open-ended tasks** with multiple valid answers. An alternative direction focuses on making Best-of-N sampling adaptive by learning when to stop generating candidates based on **reward model feedback** (Cobbe et al., 2021; OpenAI, 2022; Zhang et al., 2024). While these adaptive BoN methods show effectiveness across diverse scenarios, they rely on data-centric, training-heavy pipelines to learn auxiliary stopping models (Damani et al., 2025), which limits adaptability to new domains while potentially introducing bias and reducing output diversity. Critically, both approaches rely on heuristics or learned approximations without theoretical guarantees of optimality, making their stopping decisions inherently ad-hoc.

To bridge this theory-practice gap, we leverage principles in Bayesian optimal stopping (Baucells and Zorc, 2024) and reformulate LLM sampling as a sequential search problem. This framework ensures stopping decisions achieve **Bayesian optimality** given currently observed data, eliminating reliance on heuristic approximations (Rothschild, 1974). Rather than learning reward distributions *offline*, we conceptualize them as latent processes for online updating: each generated response reveals



Figure 1: **Comparison of BEACON adaptive sampling versus Best-of-N fixed sampling.** BEACON adaptively determines sample size by learning the reward distribution and determine if additional sampling is worth the cost. Intuitively, BEACON stops earlier for consistent samples and continues sampling to find better solutions for variable reward samples, while Best-of-N always uses fixed samples (in this case, 8) regardless.

information about the underlying reward distribution while incurring computational costs (Toth and Oberhauser, 2020). The fundamental challenge becomes determining the **optimal stopping point** where expected benefits from additional samples no longer justify associated costs, which can be addressed with Bayesian learning theory (Christensen, 1986; Bikhchandani and Sharma, 1996).

We therefore introduce the **Bayesian Efficient Adaptive Criterion for Optimal N-stopping (BEACON)**, a novel adaptive sampling framework that makes optimal stopping decisions computationally practical while enabling real-time deployment without additional offline training requirements. Our approach can be understood through two synergistic components: **sequential search** addresses the adaptivity challenge, while **Bayesian learning** provides a principled framework for on-line reward distribution learning. Together, these components enable derivation of adaptive sampling policies without pre-training while guaranteeing **theoretical optimality**. BEACON sequentially collects responses, updates sufficient statistics of the posterior reward distribution, and employs an index-based sampling policy that compares a quality index against a cost threshold. Intuitively, BEACON terminates when reward evaluations exhibit minimal variation, indicating stable characterization of the quality distribution, or when additional computation is unlikely to yield superior rewards. Figure 1 contrasts BEACON’s adaptive stopping with conventional Best-of-N sampling, illustrating how our Bayesian criterion adaptively allocates computation across variable-reward queries. Our

empirical evaluations on reasoning and alignment benchmarks demonstrate that BEACON substantially reduces average inference costs compared to fixed BoN while maintaining comparable performance, with demonstrated utility for cost-effective preference data generation, practical hyperparameter selection guidance, and extensions to batch sampling for enhanced efficiency. In sum, our main contributions are: (1) We propose BEACON, an **adaptive sampling framework** that reformulates LLM sampling as a sequential Bayesian search problem for theoretically optimal stopping without training additional auxiliary models. (2) We provide rigorous analysis of its **theoretical guarantees** and computational complexity. (3) We conduct comprehensive experiments across diverse benchmarks, demonstrating its effectiveness against established baselines and highlighting practical extensions for post-training and real-world deployment.

2 Modeling LLM Sampling as Sequential Search Problem

2.1 Methodology Overview

Reward Models as Quality Assessment Tools. Reward Models (RMs) (Zhang et al., 2024; Zhong et al., 2025) provide scalar assessments of response quality that serve as evaluation signals for adaptive sampling. Trained on pairwise preference data $D = \{(x_i, y_{w,i}, y_{l,i})\}$, these models encode both preference direction and certainty in the magnitude of reward differences, making them ideal quality signals for probabilistic modeling.

Sequential Search for Optimal Stopping. We

084
085
086
087
088
089
090
091
092
093
094
095
096
097
098
099
100
101
102
103
104
105
106
107
108
109
110
111
112
113
114
115
116
117

118
119
120
121
122
123
124
125
126
127
128
129
130
131
132
133
134
135
136
137
138
139
140
141
142
143
144
145
146
147
148
149

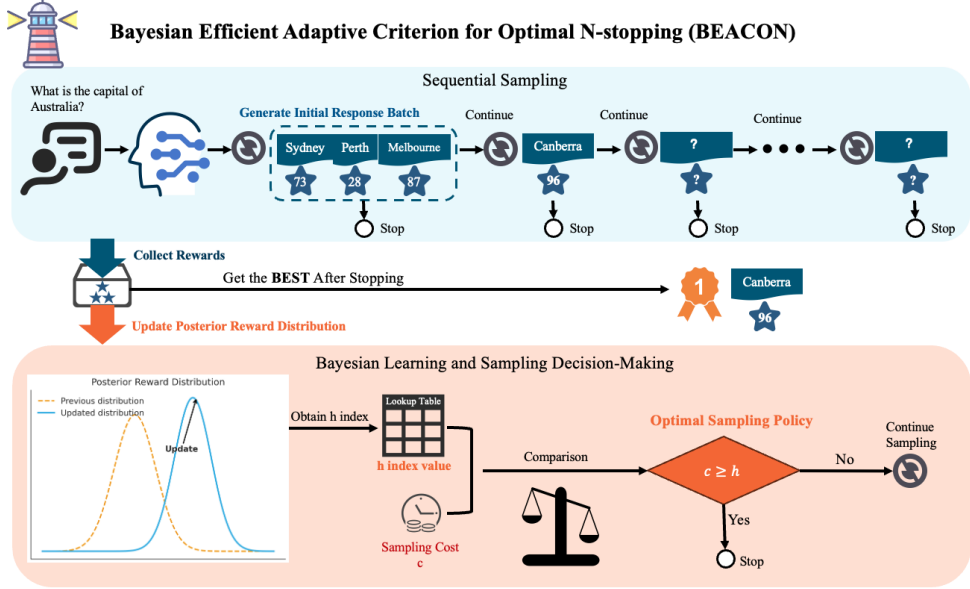


Figure 2: **BEACON framework**: The top layer shows sequential sampling of LLM responses with reward model evaluation. The bottom layer illustrates the optimal stopping mechanism, which updates Bayesian posterior beliefs about reward distribution parameters after each sample and determines when to stop based on optimal sampling policy, comparing the index-based threshold to the sampling cost.

150 reformulate LLM sampling as a sequential search
 151 problem to maximize net gain—balancing the highest quality against sampling cost. This approach
 152 replaces heuristics with theoretically grounded
 153 guarantees for deciding when additional samples are no
 154 longer economically justified. Sequential Search
 155 examines alternatives one by one, deciding after
 156 each observation whether to accept the current
 157 best outcome or continue sampling (Stigler,
 158 1961; Weitzman, 1979) (detailed in Appendix D.1).
 159 Given observed rewards $\mathbf{r}_k = \{r_1, \dots, r_k\}$ with
 160 best reward $z_k = \max\{r_1, \dots, r_k\}$ and sampling
 161 cost c per observation, the challenge is determining
 162 the optimal stopping point, identifying the maximum
 163 reward while minimizing costs. When the
 164 reward distribution is *known*, this admits closed-
 165 form solutions (Weitzman, 1979). However, LLM
 166 sampling presents the more challenging case where
 167 the underlying reward distribution is *unknown*.
 168

169 **A Principled Bayesian Framework for Unknown**
 170 **Distributions.** BEACON combines sequential
 171 search with Bayesian learning to address the funda-
 172 mental challenge of *unknown reward distributions*
 173 by learning parameters online during sam-
 174 pling, enabling zero-shot deployment without of-
 175 line training or pre-training. For computational
 176 tractability, we employ conjugate priors that en-
 177 able closed-form updates. We focus on the Nor-
 178 mal distribution for its practical utility and unique
 179 theoretical properties—it is the only continuous

180 distribution with computationally efficient optimal
 181 index policies in sequential search literature (Bau-
 182 cells and Zorc, 2024), which is more challenging
 183 than simpler, discrete conjugate families such as
 184 the beta-binomial extension that is also supported
 185 by BEACON (demonstrated in Appendix D.6).

2.2 Model Setup

186 **Problem Setting.** Given a query x and a policy
 187 LLM $\pi_\phi(y|x)$, we sequentially generate responses
 188 $\{y_1, \dots, y_k\}$ where $y_i \sim \pi_\phi(\cdot|x)$ and evaluate each
 189 using a reward model $R(x, y_i) = r_i$. The reward
 190 distribution $f(r_k|x)$ emerges from the marginal-
 191 ized distribution over the response generation and
 192 reward evaluation processes. We assume rewards
 193 follow an i.i.d. Normal distribution with unknown
 194 parameters, which distinguishes our approach from
 195 methods requiring known distributions or training
 196 auxiliary models. After collecting k samples with
 197 rewards $\mathbf{r}_k = \{r_1, \dots, r_k\}$, we denote the current
 198 best reward as $z_k = \max\{r_1, \dots, r_k\}$. Each sam-
 199 ple incurs cost c , and sampling continues up to
 200 maximum horizon n . Our objective is deter-
 201 mining the optimal stopping time K that maximizes
 202 expected net gain $\mathbb{E}[z_K - K \cdot c]$.

203 **Bayesian Learning with Conjugate Priors.** To
 204 enable tractable Bayesian updating, we employ
 205 a Normal-Inverse-Gamma (NIG) conjugate prior
 206 for unknown parameters (μ, σ^2) . Conjugate priors
 207 guarantee a fixed-dimensional state space during se-

Algorithm 1 BEACON: Bayesian Efficient Adaptive Criterion for Optimal N-stopping

Input: Query x , policy LLM $\pi_\phi(y|x)$, reward model $R(x, y)$, cost c , max samples n , grid size G
Output: Best response y^* and its reward r^*

// Step 1: Initialize prior and h-index table

1 $(\alpha_0, \nu_0, \beta_0, \mu_0) \leftarrow (-0.5, 0, 0, 0)$ ▷ Non-informative prior
2 $h\text{-table} \leftarrow \text{PrecomputeTable}(n, G, \alpha_0, \nu_0)$ ▷ Pre-compute as in §D.5

// Step 2: Generate initial samples and compute baseline parameters

3 Generate $\{y_1, y_2, y_3\} \sim \pi_\phi(y|x)$ and compute $r_i \leftarrow R(x, y_i)$ for $i \in \{1, 2, 3\}$

4 $(\alpha, \nu, \mu, \beta) \leftarrow \text{UpdateHyperParams}(r_1, r_2, r_3, \alpha_0, \nu_0, \beta_0, \mu_0)$

5 $z \leftarrow \max\{r_1, r_2, r_3\}$, $\sigma \leftarrow \sqrt{\frac{(\nu+1)\beta}{\nu\alpha}}$, $k \leftarrow 3$

// Step 3: Adaptive sampling loop

6 **while** $k < n$ **do**

7 $\hat{z} \leftarrow (z - \mu)/\sigma$, $h \leftarrow \text{LookupHIndex}(h\text{-table}, k, \hat{z})$

8 **if** $h \leq c/\sigma$ **then**

9 **break**

10 **end**

11 Generate $y_k \sim \pi_\phi(y|x)$ and compute $r_k \leftarrow R(x, y_k)$ $k \leftarrow k + 1$

12 $q_{0.01} \leftarrow F_{2\alpha_{k-1}}^{-1}(0.01|\mu, \sigma)$ $\tilde{r}_k \leftarrow \begin{cases} \mu & \text{if } r_k < q_{0.01} \\ r_k & \text{otherwise} \end{cases}$ ▷ Filter extreme low values

13 $(z, \mu, \sigma) \leftarrow \text{UpdateStats}(z, \mu, \sigma, \tilde{r}_k, k)$ ▷ The sufficient statistics updated by (5)

14 **end**

15 $i^* \leftarrow \arg \max_{i \in \{1, \dots, k\}} r_i$ **return** y_{i^*} , r_{i^*}

209 quential sampling (Diaconis and Ylvisaker, 1979),
210 essential for computational tractability. Starting
211 with prior $\text{NIG}(\mu_0, \nu_0, \alpha_0, \beta_0)$, after observing $k \geq$
212 k_0 samples (where k_0 is the minimum for well-
213 defined posteriors; see Appendix D.2), the posterior
214 parameters update according to closed-form expres-
215 sions detailed as (4) in Appendix D.2. Importantly,
216 the triple (z_k, μ_k, σ_k) forms **sufficient statistics**
217 for all observed rewards, enabling efficient state
218 representation where the updating formula (5) in
219 Appendix D.3 shows how these statistics evolve
220 with each new sample.

221 **Bellman Equation.** To formulate our objective
222 function $\mathbb{E}[z_K - K \cdot c]$ in Bellman equation as:

223

$$V_{n,k}(z_k, \mu_k, \sigma_k; c) = \max\{z_k, \mathbb{E}[V_{n,k+1}(z_{k+1}, \mu_{k+1}, \sigma_{k+1}; c)] - c\}, \quad (1)$$

224 with corresponding optimal stopping rule:

225

$$\text{Stop iff } H_{n,k}(z_k, \mu_k, \sigma_k; c) = \mathbb{E}[V_{n,k+1}(z_{k+1}, \mu_{k+1}, \sigma_{k+1}; c)] - z_k \leq c. \quad (2)$$

226 where $H_{n,k}$ represents the expected marginal gain
227 from continued sampling.

2.3 Optimal Sampling Policy

Building on recent theoretical advances of the computationally efficient Universal Index Policy (Baucells and Zorc, 2024), we can establish an efficient criterion for optimal stopping decisions.

Definition 1. For $k_0 \leq k < n$, the *h-index function* $h_{n,k} : \mathbb{R} \rightarrow (0, \infty)$ maps each standardized best reward $\hat{z} \in \mathbb{R}$ to the unique value $c > 0$ that solves the condition where the expected marginal gain from continuing equals the sampling cost.

Theorem 1 (Optimal Sampling Policy). After generating initial samples $\{y_1, y_2, \dots, y_{k_0}\}$ to establish valid posterior parameters, the optimal Bayesian policy at each step $k \geq k_0$ is to continue sampling if and only if:

$$h_{n,k} \left(\frac{z_k - \mu_k}{\sigma_k} \right) > \frac{c}{\sigma_k} \quad (3)$$

The stopping time $K = \min\{k \geq k_0 : h_{n,k}(\hat{z}_k) \leq c/\sigma_k\} \wedge n$ maximizes the expected net gain $\mathbb{E}[z_K - K \cdot c]$.

The proof of Theorem 1 is provided in the Appendix. Our approach standardizes the current best

249 reward $\hat{z}_k = (z_k - \mu_k)/\sigma_k$, retrieves the corre-
250 sponding h-index value, and compares it against
251 the cost-adjusted threshold c/σ_k . The algorithm
252 stops when this threshold is no longer exceeded,
253 indicating that further sampling has become eco-
254 nomically inefficient given our posterior beliefs.

255 **Normality Assumption.** While exact optimality
256 guarantees hold under normality, BEACON re-
257 mains robust to moderate distributional violations
258 through several mechanisms: (1) the Central Limit
259 Theorem suggests that reward signals naturally ap-
260 proximate normality in practice (as shown in App.
261 E.5); (2) our focus on identifying maximum re-
262wards depends on the right tail of the distribution,
263 making the framework less sensitive to left-tail de-
264 viations; and (3) we introduce a robust updating
265 mechanism (see Section 3.2) that filters extreme
266 low outliers while preserving high-quality samples,
267 maintaining practical effectiveness when distribu-
268 tions exhibit negative skewness.

269 **Sensitivity Analysis.** The optimal stopping time
270 K exhibits intuitive dependencies on key problem
271 parameters. When sampling cost c increases, ex-
272 ploration is often discouraged. If the current best
273 reward z_k substantially exceeds the posterior mean
274 μ_k (large \hat{z}_k), the framework recognizes an excep-
275 tionally high-quality sample has likely been found
276 and stops earlier. Conversely, greater posterior un-
277 certainty (larger σ_k) encourages continued sam-
278 pling through two mechanisms: by decreasing the
279 normalized score \hat{z}_k and lowering the effective cost
280 threshold $\frac{c}{\sigma_k}$. Intuitively, when more exploration
281 budget remains available (larger $n - k$), the algo-
282 rithm tends to be more patient, balancing immediate
283 rewards against future exploration potential (see
284 Appendix D.8 for proofs and formal statements).

285 2.4 BEACON Framework

286 **Hyperparameter Configuration.** BEACON re-
287 quires three key hyperparameters that jointly de-
288 fine the optimization framework: (1) *Prior Pa-
289 rameters* – We use Jeffreys’ non-informative prior
290 $(\alpha_0, \nu_0, \mu_0, \beta_0) = (-0.5, 0, 0, 0)$ for task-agnostic
291 deployment without domain-specific calibration, re-
292quiring $k_0 = 3$ initial samples for well-defined pos-
293 teriors (Appendix D.2); (2) *Maximum Horizon* (n) –
294 The sampling budget follows standard Best-of-N
295 configurations (e.g. $n \in \{8, 16, 32\}$), where larger
296 horizons increase patience but raise h-index pre-
297 computation costs (Appendix D.5); (3) *Sampling
298 Cost* (c) – Controls the quality-efficiency trade-off,

299 with higher values favoring efficiency and lower
300 values favoring quality.

301 **Algorithm Implementation.** Algorithm 1 presents
302 the complete BEACON procedure, with the overall
303 framework illustrated in Figure 2. After initializing
304 Jeffreys’ non-informative priors and pre-computing
305 h-index tables, we generate $k_0 = 3$ bootstrap sam-
306 ples to establish valid posterior parameters. The
307 adaptive sampling loop then iteratively: (1) com-
308putes standardized score $\hat{z}_k = (z_k - \mu_k)/\sigma_k$; (2)
309 retrieves h-index $h_{n,k}(\hat{z}_k)$ via table lookup; (3) ap-
310plies optimal stopping criterion $h_{n,k}(\hat{z}_k) \leq c/\sigma_k$;
311 and (4) if continuing, generates new samples and
312 updates parameters using robust filtering. This de-
313sign transforms computationally intensive Bellman
314 optimization into efficient table lookups, enabling
315 real-time deployment while maintaining theoretical
316 optimality guarantees.

317 **Computational Complexity.** BEACON’s compu-
318 tational overhead consists of two distinct compo-
319 nents with different scalability characteristics: (1)
320 *h-Table Pre-computation* – Constructing the lookup
321 table $h_{n,k}(\cdot)$ requires $\mathcal{O}(nG)$ operations for hori-
322 zon n and grid resolution G . This one-time cost
323 is amortized across all queries that share the same
324 horizon, making it negligible in multi-query de-
325 ployments. When tasks involve multiple horizons
326 $\{n_1, \dots, n_J\}$, complexity grows only with the
327 number of distinct horizon values rather than the
328 total number of queries; (2) *Sequential Inference*
329 – Each query entails sequential decision-making,
330 where samples are generated one-by-one to update
331 posterior beliefs. This inherent dependency limits
332 within-query parallelization and can increase la-
333 tency relative to batch-generation methods. Never-
334 theless, the cost can be partially mitigated through
335 batch-parallel sampling (Section 3.2).

336 3 Experiments

337 3.1 Main Results

338 **Setup.** We use a warm-start of $k_0 = 3$ (to initialize
339 a Jeffreys’ prior) and maximum horizon of $n = 32$
340 (standard for Best-of-N (Singhi et al., 2025)). For
341 each method m , K_m denotes its realized sample
342 count ($1 \leq K_m \leq n$) and \bar{K}_m its dataset av-
343 erage. We focus comparisons on training-free
344 methods and standard BoN as these represent the
345 most widely deployed approaches. Specifically, we
346 include one-shot **Chain-of-Thought** (CoT) with
347 $K=1$; **Self-Consistency** (SC) (Wang et al., 2022)

Table 1: Comparison of BEACON with baseline sampling methods across different models and tasks. BEACO achieves a superior trade-off between Accuracy/Win Rate/Reward \bar{z}_K and efficiency (Avg Sample \bar{K}), measured by the implicitly optimized objective \hat{V}_K . Upward arrows (\uparrow) indicate percentage improvement in accuracy or win rate over CoT baselines; downward arrows (\downarrow) show percentage reduction in samples compared to the maximum BoN sample size (32). **Reward models:** **N-RM** uses *Llama-3.1-Nemotron-70B-Reward* (Wang et al., 2025c); **S-RM** uses *Skywork-Llama-3.1-8B* (Liu et al., 2024); Additional runs for statistical significance reported in Table 6.

Model	Method	Reasoning Tasks (Avg. MATH/AIME/AMC)				Alignment Task (AlpacaEval 2.0)			
		Accuracy \uparrow (%)	Samples \downarrow (\bar{K})	Reward \uparrow (\bar{z}_K)	Value \uparrow (\hat{V}_K)	Win Rate \uparrow (%)	Samples \downarrow (\bar{K})	Reward \uparrow (\bar{z}_K)	Value \uparrow (\hat{V}_K)
LLaMA-3.2-3B	Direct CoT	20.0	1.0	-1.15	-0.40	16.0	1.0	-1.08	-0.80
	SC	28.5 \uparrow 42.5%	16.0 \downarrow 50.0%	-0.35	-0.01	-	-	-	-
	RASC	27.8 \uparrow 39.0%	5.2 \downarrow 83.8%	-0.30	0.66	20.0 \uparrow 25.0%	7.0 \downarrow 78.1%	-1.12	-0.55
	AS	27.8 \uparrow 39.0%	5.6 \downarrow 82.5%	-0.31	0.62	-	-	-	-
	BoN (N-RM)	33.4 \uparrow 67.0%	32.0	1.75	0.29	25.0 \uparrow 56.3%	32.0	1.76	0.80
	BoN (S-RM)	31.0 \uparrow 55.0%	32.0	1.72	0.25	24.0 \uparrow 50.0%	32.0	1.65	0.55
	BEACON (N-RM)	32.8 \uparrow 64.0%	15.8 \downarrow 50.6%	1.68	1.12	23.5 \uparrow 46.9%	14.5 \downarrow 54.7%	1.68	1.20
	BEACON (S-RM)	32.0 \uparrow 60.0%	16.1 \downarrow 49.7%	1.66	1.08	22.5 \uparrow 40.6%	14.8 \downarrow 53.8%	1.53	1.15
Qwen2.5-7B	Direct CoT	43.0	1.0	-1.25	-0.53	22.5	1.0	-0.85	-0.53
	SC	50.0 \uparrow 16.3%	16.0 \downarrow 50.0%	-0.37	-0.02	-	-	-	-
	RASC	49.5 \uparrow 15.1%	4.3 \downarrow 86.6%	-0.28	0.57	25.0 \uparrow 11.1%	4.0 \downarrow 87.5%	-1.15	-0.30
	AS	49.3 \uparrow 14.7%	4.6 \downarrow 85.6%	-0.29	0.55	-	-	-	-
	BoN (N-RM)	55.2 \uparrow 28.4%	32.0	1.85	0.09	36.0 \uparrow 60.0%	32.0	2.02	1.02
	BoN (S-RM)	55.0 \uparrow 27.9%	32.0	1.76	0.05	35.0 \uparrow 55.6%	32.0	2.05	1.05
	BEACON (N-RM)	54.0 \uparrow 25.6%	6.5 \downarrow 79.7%	1.78	0.92	33.5 \uparrow 48.9%	7.8 \downarrow 75.6%	1.95	1.55
	BEACON (S-RM)	54.0 \uparrow 25.6%	7.0 \downarrow 78.1%	1.64	0.91	33.0 \uparrow 46.7%	8.0 \downarrow 75.0%	1.90	1.50
Grok-3-Mini	Direct CoT	89.0	1.0	-1.10	-0.28	82.0	1.0	-0.98	-0.70
	SC	92.0 \uparrow 3.4%	16.0 \downarrow 50.0%	-0.38	-0.04	-	-	-	-
	RASC	93.8 \uparrow 5.4%	3.5 \downarrow 89.1%	-0.22	0.56	85.5 \uparrow 4.3%	3.5 \downarrow 89.1%	-1.02	-0.55
	AS	93.8 \uparrow 5.4%	3.8 \downarrow 88.1%	-0.23	0.53	-	-	-	-
	BoN (N-RM)	95.5 \uparrow 7.3%	32.0	1.62	0.10	94.0 \uparrow 14.6%	32.0	1.45	0.80
	BoN (S-RM)	95.0 \uparrow 6.7%	32.0	1.70	0.19	94.2 \uparrow 14.9%	32.0	1.42	0.79
	BEACON (N-RM)	94.8 \uparrow 6.5%	5.0 \downarrow 84.4%	1.57	0.99	92.8 \uparrow 13.2%	4.0 \downarrow 87.5%	1.39	1.94
	BEACON (S-RM)	94.2 \uparrow 5.8%	5.5 \downarrow 82.8%	1.64	0.95	93.4 \uparrow 13.9%	4.3 \downarrow 86.6%	1.36	1.93

Note: SC = Self-Consistency (Wang et al., 2022); RASC = Reasoning-Aware Self-Consistency (Wan et al., 2025a);

AS = Adaptive Sampling (Aggarwal et al., 2023); BoN = Best-of- N sampling (Cobbe et al., 2021) SC and AS are not applicable to alignment tasks.

348 with majority vote over n samples; **Adaptive-**
349 **Consistency** (AS) (Aggarwal et al., 2023), a model-
350 agnostic method that fits a Dirichlet–multinomial
351 posterior to agreement patterns for early stopping;
352 **RASC** (Wan et al., 2025a), a heuristic adaptive
353 sampler using CoT quality scores; and Best-of- N
354 (**BoN**), which selects the highest reward-scored
355 candidate from n attempts. Policy models in-
356 clude LLaMA-3.2-8B, Qwen2.5-7B-Instruct, and
357 Grok-3-mini; reward models include Llama-3.1-
358 Nemotron-70B-Reward and Skywork-Llama-3.1-
359 8B. We used CoT (Wei et al., 2022) prompting
360 with model-specific templates. Evaluation cov-
361 ered: (1) Pass @ 1 for *Reasoning Tasks* on three
362 mathematical benchmarks (MATH-500 (Lightman
363 et al., 2023), AIME24 (Mathematical Asso-
364 ciation of America, 2024), AMC23); (2) *Alignment*
365 *Task* using AlpacaEval 2.0 (Li et al., 2023),
366 comparing responses for user instructions against
367 GPT-4; and (3) for both tasks, *expected standard-
368 ized reward* \bar{z}_K and *expected standardized value*
369 $\hat{V}_K = \mathbb{E}[z_K - K \cdot c]$, representing the quality-
370 efficiency tradeoff (more details in Appendix A.1).

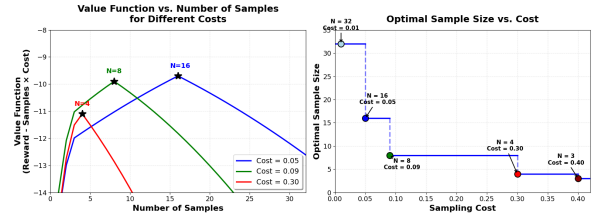


Figure 3: Impact of the sampling cost (c) on the value optimization and the optimal sample size. Higher c results in earlier stopping to reach Bayesian optimality.

Optimal Performance-Efficiency Tradeoff. Table 1 demonstrates BEACON’s ability to achieve an optimal balance between performance and computational efficiency. Our approach consistently matches BoN’s performance while requiring significantly fewer samples. This tradeoff is quantitatively validated by *consistently superior value function scores*, confirming that BEACON effectively maximizes expected net gain as a Bayesian optimal stopping solution. Results remain consistent across experimental conditions—including different base models, reward models, and task categories.

Impact of Sampling Cost (c) on Optimized Sam-

371
372
373
374
375
376
377
378
379
380
381
382
383

ple Size. We analyze how the sampling cost parameter c shapes BEACON’s adaptive sample size K_{BEACON} . As shown in Figure 3, increasing c consistently reduces the optimal number of samples, aligning with our discussion in Section 2.2. Unlike factors such as reward variance, response quality, or remaining budget—which emerge from query characteristics— c serves as a *human-interpretable* control knob for balancing efficiency and quality. Stopping typically occurs when responses stabilize, when quality remains uniformly low, or when nearing the maximum budget (examples in E.5). For practical deployment, we recommend a default $c = 0.1$ when there is no strong preference between efficiency and quality. Lower values of c are better suited for difficult, high-variance tasks, whereas higher values suit easier or consistent ones (See App. B.1 for guidelines).

BEACON’s Effectiveness at Controlled Average Sample Sizes.

Building on our analysis of how sampling cost c influences BEACON’s stopping behavior, we provide an alternative perspective by investigating scenarios where c is calibrated to ensure BEACON’s average sample size (\bar{K}_{BEACON}) matches the fixed sample size of standard Best-of-N (BoN) strategies. Figure 4 illustrates this controlled comparison, revealing BEACON’s advantages: (1) when using the *same number of samples* ($\bar{K}_{BEACON} = K_{BoN}$), BEACON achieves substantially *higher accuracy and reward*; and (2) BEACON can maintain *equivalent accuracy and reward* while requiring *fewer samples*. This performance advantage stems from BEACON’s dynamic sampling strategy, which intelligently invests additional samples in promising queries while terminating earlier for less promising ones—a fundamental improvement over BoN’s uniform sampling approach that allocates identical resources regardless of query nature or potential quality improvements.

3.2 Extensions and Applications

Efficiency in Data Generation for Iterative DPO.

To demonstrate BEACON’s practical utility, we applied it to improve efficiency in data generation for Iterative Direct Preference Optimization (DPO) (Rafailov et al., 2023), which enhances LLM consistency on challenging questions (Xiong et al., 2025). We evaluated BEACON against a standard Best-of-N (BoN) approach—the conventional method for generating preference pairs in iterative training processes (Yuan et al., 2025); comprehensive experimental details are provided in

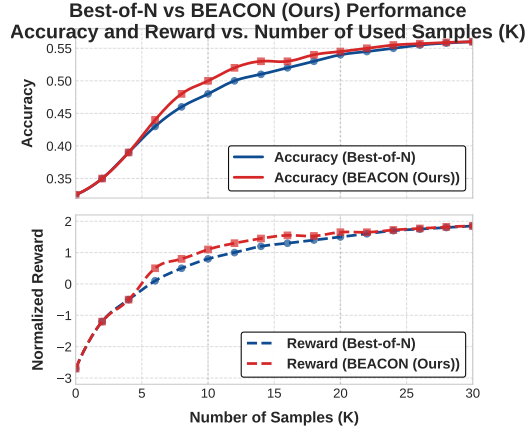


Figure 4: **Comparative performance trajectories on Best-of-N vs. BEACON.** When forcing the same number of samples, BEACON achieves better performance; When restricting on a threshold performance, BEACON would require less number of samples.

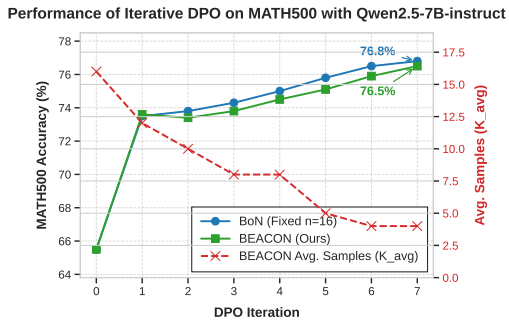


Figure 5: Iterative DPO performance on MATH500 with Qwen2.5-7B-instruct. BEACON (accuracy: green squares) achieves competitive accuracy relative to BoN (fixed $n=16$, accuracy: blue circles) across seven DPO iterations while reducing the average number of samples required per prompt (\bar{K} : red dashed line, right y-axis).

Appendix C.2. Figure 5 illustrates performance across seven DPO iterations, revealing that BEACON achieved *comparable accuracy* while progressively reducing the average required samples (\bar{K} , shown on the secondary y-axis). This preliminary experiment demonstrates that as LLMs become more consistent and aligned with preferences, BEACON efficiently identifies high-quality preference pairs with substantially fewer samples to improve post-training efficiency.

Robust Updating for Negative Skewness. Reward distributions from LLMs occasionally exhibit negative skewness (Fig 7), where extreme low outliers distort posterior updates. We introduce a *robust updating mechanism* that preserves the informative right tail—critical for identifying maximum rewards—while mitigating left-tail outliers. Values below the 1% posterior-predictive quantile are

Table 2: Batch-parallel BEACON performance across different batch sizes, evaluated with LLaMA 3.2 on a mathematical reasoning dataset. Memory overhead is measured relative to sequential execution ($b = 1$).

Batch Size	Speedup (vs Seq.)	Memory Overhead	Acc. Change	Avg. Samples
1 (Seq.)	1.00×	Baseline	0.0%	15.8
2	1.65×	+12%	+0.2%	16.1
4	2.31×	+28%	+0.6%	17.2
8	2.85×	+65%	+0.8%	19.4

replaced with the current posterior mean, ensuring high-quality candidates remain intact while the posterior better reflects the reward landscape. This adaptive update reduces outlier impact without violating Gaussian assumptions. Figure 9 shows the robust mechanism consistently drives BEACON’s stopping points closer to the true optimum. Full derivations and analysis are in Appendix E.4.

Parallel Sampling. While BEACON is inherently sequential, practical deployments can benefit from batch-parallel sampling, like BoN Sampling, to reduce wall-clock time at the expense of higher memory usage. In this mode, BEACON generates batches of b samples simultaneously, *updates posterior beliefs after each batch*, and applies the same stopping criterion $h_{n,k}(\hat{z}_k) \leq \frac{c}{\sigma_k}$, where k now indexes completed batches. Within each batch, responses are sampled independently using the same prompt, then evaluated with the reward model; posterior parameters are updated with all batch rewards, and the stopping rule is applied. Termination selects the highest-reward response across all batches. As shown in Table 2, batching can slightly improve accuracy since larger batches enforce a minimum exploration depth before each stopping decision, though this comes with diminishing returns and increased memory overhead. Moreover, as discussed in 2.4, BEACON’s pre-computed UIP index tables can be *reused across multiple parallel queries* without recompilation, enabling efficient query-level parallelization at no additional cost.

4 Related Work

Parallel Reasoning and Efficiency. Parallel scaling approaches (Zeng et al., 2025; Qian et al., 2025) enhance LLM answers by generating multiple candidates and aggregating them into a final answer, through consensus (e.g., majority voting and weighted confidence scores (Wang et al., 2022; Chen et al., 2024; Fu et al., 2025)) or with external verifiers and reward models that rank and

select superior solutions (Cobbe et al., 2021; Ichihara et al., 2025; Zhang et al., 2024; Ankner et al., 2024). While effective, these methods prioritize response quality without explicitly addressing computational costs. Recent work on efficient sampling strategies (Sui et al., 2025; Fu et al., 2024) seeks to address the issue using fine-tuned verifiers (Manvi et al., 2024; Huang et al., 2025; Wan et al., 2025a) or heuristic rules that adapt resource allocation by query complexity (Wang et al., 2025b; Wan et al., 2025b; Aggarwal et al., 2023). In contrast, our BEACON framework takes a principled Bayesian learning approach that integrates reward signals with optimal stopping theory to jointly optimize response quality and computational efficiency.

Bandits and Bayesian Optimization. BEACON’s sequential search framework connects to established paradigms in decision theory and optimization (Keith and Ahner, 2021). While Multi-Armed Bandit problems (Lattimore and Szepesvári, 2020; Slivkins, 2019) emphasize maximizing cumulative rewards, BEACON focuses on finding the maximum reward with minimal sampling. Our work builds more directly on best-arm identification (Audibert and Bubeck, 2010; Gabilon et al., 2012) and Extreme Bandits (Carpentier and Valko, 2014; Lopez et al., 2021), which similarly target optimal or extreme-value outcomes. BEACON’s novelty lies in combining a Bayesian approach with conjugate priors for adaptive belief updates and optimal stopping theory (Ferguson, 2012) to decide when further exploration is no longer cost-effective. While conceptually related to budgeted bandits (Xia et al., 2016) and Bayesian optimization (Shahriari et al., 2015), BEACON applies these ideas to LLM sample efficiency, bridging theoretical insights with practical inference.

5 Conclusion

We introduced **BEACON**, a principled framework grounded in sequential search theory with Bayesian learning under conjugate priors. BEACON addresses the fundamental trade-off between computational cost and response quality during LLM inference by dynamically determining when to stop sampling based on evolving posterior beliefs about reward distributions and the cost of additional sampling. With strong empirical results and comprehensive theoretical analysis, we demonstrate the value of decision-theoretic approaches for resource-aware scaling in LLM reasoning and generation.

543 Limitations

544 While BEACON provides strong efficiency gains,
545 several avenues remain for extending the frame-
546 work. First, BEACON’s optimality guarantees
547 assume the reward model provides accurate qual-
548 ity signals; systematic reward model miscalibra-
549 tion could lead to suboptimal stopping decisions.
550 Integrating reward model uncertainty quantifica-
551 tion—for instance, by incorporating ensemble-
552 based confidence estimates into the posterior up-
553 dates—represents a promising direction for enhanc-
554 ing robustness. Second, the framework currently
555 assumes independence across samples, whereas ex-
556 ploiting correlations between generated responses
557 (e.g., through shared reasoning patterns) could fur-
558 ther improve sample efficiency.

559 Future research can address these opportunities
560 by extending BEACON to leverage reward model
561 ensembles for uncertainty-aware stopping and in-
562 corporating structured priors that capture depen-
563 dencies between samples. Furthermore, our prelimi-
564 nary experiments with Iterative DPO (Section 3.2)
565 suggest BEACON’s potential for post-training op-
566 timization, warranting deeper investigation into its
567 role across different training paradigms and reward
568 model architectures. Additionally, dynamic tuning
569 of the cost parameter c based on query character-
570 istics could enable fully automated adaptation to
571 varying computational budgets. Together, these
572 directions position BEACON as a foundation for
573 both efficient inference and adaptive post-training
574 pipelines in production deployments.

575 References

576 Pranjal Aggarwal, Aman Madaan, Yiming Yang, and
577 Mausam. 2023. [Let’s sample step by step: Adaptive-
578 consistency for efficient reasoning and coding with
579 LLMs](#). In *Proceedings of the 2023 Conference on
580 Empirical Methods in Natural Language Process-
581 ing*, pages 12375–12396, Singapore. Association for
582 Computational Linguistics.

583 Zachary Ankner, Mansheej Paul, Brandon Cui,
584 Jonathan Daniel Chang, and Prithviraj Ammanabrolu.
585 2024. [Critique-out-loud reward models](#). In *Pluralis-
586 tic Alignment Workshop at NeurIPS 2024*.

587 Jean-Yves Audibert and Sébastien Bubeck. 2010. Best
588 arm identification in multi-armed bandits. In *Pro-
589 ceedings of the 23rd Conference on Learning Theory
(COLT)*, pages 41–53.

590 Manel Baucells and Saša Zorc. 2024. Search in the
591 dark: The case with recall and gaussian learning.
592 *Operations Research*.

593 Sushil Bikhchandani and Sunil Sharma. 1996. Optimal
594 search with learning. *Journal of Economic Dynamics
595 and Control*, 20(1):333–359.

596 Alexandra Carpentier and Michal Valko. 2014. Extreme
597 bandits. In *Advances in Neural Information Process-
598 ing Systems*, volume 27.

599 Xinyun Chen, Renat Aksitov, Uri Alon, Jie Ren, Kefan
600 Xiao, Pengcheng Yin, Sushant Prakash, Charles Sutton,
601 Xuezhi Wang, and Denny Zhou. 2024. [Universal
602 self-consistency for large language models](#). In *ICML
603 2024 Workshop on In-Context Learning*.

604 Ronald Christensen. 1986. Finite stopping in sequential
605 sampling without recall from a dirichlet process. *The
606 Annals of Statistics*, pages 275–282.

607 Karl Cobbe, Vineet Kosaraju, Mohammad Bavarian,
608 Mark Chen, Heewoo Jun, Lukasz Kaiser, Matthias
609 Plappert, Jerry Tworek, Jacob Hilton, Reichiro
610 Nakano, Christopher Hesse, and John Schulman.
611 2021. [Training verifiers to solve math word prob-
612 lems](#). *Preprint*, arXiv:2110.14168.

613 Mehul Damani, Idan Shenfeld, Andi Peng, Andreea
614 Bobu, and Jacob Andreas. 2025. [Learning how hard
615 to think: Input-adaptive allocation of LM computa-
616 tion](#). In *The Thirteenth International Conference on
617 Learning Representations*.

618 Persi Diaconis and Donald Ylvisaker. 1979. Conju-
619 gate priors for exponential families. *The Annals of
620 statistics*, pages 269–281.

621 Thomas S. Ferguson. 2012. [Optimal stopping and appli-
622 cations](#). Lecture notes, UCLA Department of Statistics
623 Papers.

624 Yichao Fu, Junda Chen, Siqi Zhu, Zheyu Fu, Zhong-
625 dongming Dai, Aurick Qiao, and Hao Zhang. 2024.
626 [Efficiently serving llm reasoning programs with cer-
627 tainindex](#). *arXiv preprint arXiv:2412.20993*.

628 Yichao Fu, Xuewei Wang, Yuandong Tian, and Jiawei
629 Zhao. 2025. Deep think with confidence. *arXiv
630 preprint arXiv:2508.15260*.

631 Victor Gabillon, Mohammad Ghavamzadeh, and
632 Alessandro Lazaric. 2012. Best arm identification: A
633 unified approach to fixed budget and fixed confidence.
634 In *Advances in Neural Information Processing Sys-
635 tems*, volume 25.

636 Dan Hendrycks, Collin Burns, Saurav Kadavath, Akul
637 Arora, Steven Basart, Eric Tang, Dawn Song, and Ja-
638 cob Steinhardt. 2021. Measuring mathematical prob-
639 lem solving with the math dataset. *arXiv preprint
640 arXiv:2103.03874*.

641 Chengsong Huang, Langlin Huang, Jixuan Leng, Ji-
642 acheng Liu, and Jiaxin Huang. 2025. [Efficient
643 test-time scaling via self-calibration](#). *Preprint*,
644 arXiv:2503.00031.

645

646	Yuki Ichihara, Yuu Jinnai, Tetsuro Morimura, Kenshi Abe, Kaito Ariu, Mitsuki Sakamoto, and Eiji Uchibe. 2025. <i>Evaluation of best-of-n sampling strategies for language model alignment</i> . <i>Transactions on Machine Learning Research</i> .	702
647		703
648		704
649		705
650		706
651	Zixuan Ke, Fangkai Jiao, Yifei Ming, Xuan-Phi Nguyen, Austin Xu, Do Xuan Long, Minzhi Li, Chengwei Qin, Peifeng Wang, Silvio Savarese, Caiming Xiong, and Shafiq Joty. 2025. <i>A survey of frontiers in llm reasoning: Inference scaling, learning to reason, and agentic systems</i> . <i>Preprint</i> , arXiv:2504.09037.	707
652		708
653		709
654		
655		
656		
657	Alexander J. Keith and Darryl K. Ahner. 2021. <i>A survey of decision making and optimization under uncertainty</i> . <i>Annals of Operations Research</i> , 300:319–353. Published online: 25 October 2019.	710
658		711
659		712
660		713
661	Tor Lattimore and Csaba Szepesvári. 2020. <i>Bandit Algorithms</i> . Cambridge University Press.	714
662		715
663		716
664		717
665		718
666		719
667		
668		
669	Xuechen Li, Tianyi Zhang, Yann Dubois, Rohan Taori, Ishaan Gulrajani, Carlos Guestrin, Percy Liang, and Tatsunori B. Hashimoto. 2023. Alpacaeval: An automatic evaluator of instruction-following models. https://github.com/tatsu-lab/alpaca_eval .	720
670		721
671		722
672		
673		
674	Hunter Lightman, Vinit Kosaraju, Yura Burda, Harri Edwards, Bowen Baker, Teddy Lee, Jan Leike, John Schulman, Ilya Sutskever, and Karl Cobbe. 2023. <i>Let’s verify step by step</i> . <i>Preprint</i> , arXiv:2305.20050.	723
675		724
676		725
677		726
678		727
679	Chris Yuhao Liu, Liang Zeng, Jiacai Liu, Rui Yan, Jujie He, Chaojie Wang, Shuicheng Yan, Yang Liu, and Yahui Zhou. 2024. <i>Skywork-reward: Bag of tricks for reward modeling in llms</i> . <i>Preprint</i> , arXiv:2410.18451.	728
680		729
681		
682		
683	Romain Lopez, Inderjit S Dhillon, and Michael I Jordan. 2021. Learning from extreme bandit feedback. In <i>Proceedings of the AAAI Conference on Artificial Intelligence</i> , volume 35, pages 8732–8740.	730
684		731
685		732
686		733
687		734
688		735
689	Potsawee Manakul, Adian Liusie, and Mark Gales. 2023. <i>SelfcheckGPT: Zero-resource black-box hallucination detection for generative large language models</i> . In <i>The 2023 Conference on Empirical Methods in Natural Language Processing</i> .	736
690		737
691		738
692	Rohin Manvi, Anikait Singh, and Stefano Ermon. 2024. <i>Adaptive inference-time compute: Llms can predict if they can do better, even mid-generation</i> . <i>Preprint</i> , arXiv:2410.02725.	739
693		
694		
695	Mathematical Association of America. 2024. <i>American invitational mathematics examination - AIME</i> . Mathematics Competition. Accessed: May 2025.	740
696		741
697		742
698		743
699		744
700		745
701		
702	Rafael Rafailov, Archit Sharma, Eric Mitchell, Stefano Ermon, Christopher D. Manning, and Chelsea Finn. 2023. <i>Direct preference optimization: Your language model is secretly a reward model</i> . <i>ArXiv</i> , abs/2305.18290.	706
703		
704		
705		
706		
707	Michael Rothschild. 1974. Searching for the lowest price when the distribution of prices is unknown. <i>Journal of Political Economy</i> , 82(4):689–711.	707
708		708
709		709
710	Bobak Shahriari, Kevin Swersky, Ziyu Wang, Ryan P Adams, and Nando De Freitas. 2015. Taking the human out of the loop: A review of bayesian optimization. <i>Proceedings of the IEEE</i> , 104(1):148–175.	710
711		711
712		712
713		713
714	Nishad Singhi, Hritik Bansal, Arian Hosseini, Aditya Grover, Kai-Wei Chang, Marcus Rohrbach, and Anna Rohrbach. 2025. <i>When to solve, when to verify: Compute-optimal problem solving and generative verification for llm reasoning</i> . <i>Preprint</i> , arXiv:2504.01005.	714
715		715
716		716
717		717
718		718
719		719
720	Aleksandrs Slivkins. 2019. Introduction to multi-armed bandits. <i>Foundations and Trends in Machine Learning</i> , 12(1-2):1–286.	720
721		721
722		722
723	Charlie Victor Snell, Jaehoon Lee, Kelvin Xu, and Aviral Kumar. 2025. <i>Scaling LLM test-time compute optimally can be more effective than scaling parameters for reasoning</i> . In <i>The Thirteenth International Conference on Learning Representations</i> .	723
724		724
725		725
726		726
727		727
728	George J. Stigler. 1961. <i>The economics of information</i> . <i>Journal of Political Economy</i> , 69(3):213–225.	728
729		729
730	Yang Sui, Yu-Neng Chuang, Guanchu Wang, Jiamu Zhang, Tianyi Zhang, Jiayi Yuan, Hongyi Liu, Andrew Wen, Shaochen (Henry) Zhong, Hanjie Chen, and Xia Hu. 2025. <i>Stop overthinking: A survey on efficient reasoning for large language models</i> . <i>arXiv preprint arXiv:2503.16419v3</i> .	730
731		731
732		732
733		733
734		734
735		735
736	Amir Taubenfeld, Tom Sheffer, Eran Ofek, Amir Feder, Ariel Goldstein, Zorik Gekhman, and Gal Yona. 2025. <i>Confidence improves self-consistency in llms</i> . <i>Preprint</i> , arXiv:2502.06233.	736
737		737
738		738
739		739
740	Csaba Toth and Harald Oberhauser. 2020. <i>Bayesian learning from sequential data using Gaussian processes with signature covariances</i> . In <i>Proceedings of the 37th International Conference on Machine Learning</i> , volume 119 of <i>Proceedings of Machine Learning Research</i> , pages 9548–9560. PMLR.	740
741		741
742		742
743		743
744		744
745		745
746	Guangya Wan, Yuqi Wu, Jie Chen, and Sheng Li. 2025a. <i>Reasoning aware self-consistency: Leveraging reasoning paths for efficient LLM sampling</i> . In <i>Proceedings of the 2025 Conference of the Nations of the Americas Chapter of the Association for Computational Linguistics: Human Language Technologies (Volume 1: Long Papers)</i> , pages 3613–3635, Albuquerque, New Mexico. Association for Computational Linguistics.	746
747		747
748		748
749		749
750		750
751		751
752		752
753		753
754		754

755	Guangya Wan, Yuqi Wu, Hao Wang, Shengming Zhao, Jie Chen, and Sheng Li. 2025b. Derailer-rerailer: Adaptive verification for efficient and reliable language model reasoning. <i>Preprint</i> , arXiv:2408.13940.	809
756		810
757		811
758		812
759	Xinglin Wang, Shaoxiong Feng, Yiwei Li, Peiwen Yuan, Yueqi Zhang, Chuyi Tan, Boyuan Pan, Yao Hu, and Kan Li. 2025a. Make every penny count: Difficulty-adaptive self-consistency for cost-efficient reasoning. In <i>Findings of the Association for Computational Linguistics: NAACL 2025</i> , pages 6904–6917, Albuquerque, New Mexico. Association for Computational Linguistics.	813
760		814
761		815
762		816
763		817
764		818
765		819
766		820
767	Xuezhi Wang, Jason Wei, Dale Schuurmans, Quoc Le, Ed Chi, Sharan Narang, Aakanksha Chowdhery, and Denny Zhou. 2022. Self-consistency improves chain of thought reasoning in language models. <i>Preprint</i> , arXiv:2203.11171.	821
768		822
769		823
770		824
771		825
772	Yiming Wang, Pei Zhang, Siyuan Huang, Baosong Yang, Zhuseng Zhang, Fei Huang, and Rui Wang. 2025b. Sampling-efficient test-time scaling: Self-estimating the best-of-n sampling in early decoding. <i>Preprint</i> , arXiv:2503.01422.	826
773		827
774		828
775		829
776		830
777	Zhilin Wang, Alexander Bukharin, Olivier Delalleau, Daniel Egert, Gerald Shen, Jiaqi Zeng, Oleksii Kuchaiiev, and Yi Dong. 2025c. Helpsteer2-preference: Complementing ratings with preferences. In <i>The Thirteenth International Conference on Learning Representations</i> .	831
778		832
779		833
780		834
781		835
782		836
783	Jason Wei, Xuezhi Wang, Dale Schuurmans, Maarten Bosma, brian ichter, Fei Xia, Ed H. Chi, Quoc V Le, and Denny Zhou. 2022. Chain of thought prompting elicits reasoning in large language models. In <i>Advances in Neural Information Processing Systems</i> .	837
784		838
785		839
786		840
787		841
788	Martin L. Weitzman. 1979. Optimal search for the best alternative. <i>Econometrica</i> , 47(3):641–654.	842
789		843
790	Yingce Xia, Tao Qin, Weidong Ma, Nenghai Yu, and Tie-Yan Liu. 2016. Budgeted bandit problems with continuous random costs. In <i>Asian Conference on Machine Learning</i> , pages 317–332. PMLR.	844
791		845
792		846
793		847
794	Guangxuan Xiao, Yuandong Tian, Beidi Chen, Song Han, and Mike Lewis. 2024. Efficient streaming language models with attention sinks. In <i>The Twelfth International Conference on Learning Representations</i> .	848
795		849
796		850
797		851
798		852
799	Wei Xiong, Chengshuai Shi, Jiaming Shen, Aviv Rosenberg, Zhen Qin, Daniele Calandriello, Misha Khalman, Rishabh Joshi, Bilal Piot, Mohammad Saleh, Chi Jin, Tong Zhang, and Tianqi Liu. 2025. Building math agents with multi-turn iterative preference learning. In <i>The Thirteenth International Conference on Learning Representations</i> .	853
800		854
801		855
802		856
803		857
804		858
805		859
806	Ziwei Xu, Sanjay Jain, and Mohan Kankanhalli. 2025. Hallucination is inevitable: An innate limitation of large language models. <i>Preprint</i> , arXiv:2401.11817.	860
807		861
808		862
809	Asaf Yehudai, Lilach Eden, Alan Li, Guy Uziel, Yilun Zhao, Roy Bar-Haim, Arman Cohan, and Michal Shmueli-Scheuer. 2025. Survey on evaluation of llm-based agents. <i>Preprint</i> , arXiv:2503.16416.	863
810		864
811		865
812		866
813	Weizhe Yuan, Richard Yuanzhe Pang, Kyunghyun Cho, Xian Li, Sainbayar Sukhbaatar, Jing Xu, and Jason Weston. 2025. Self-rewarding language models. <i>Preprint</i> , arXiv:2401.10020.	867
814		868
815		869
816		870
817	Zheng Yuan, Hongyi Yuan, Chengpeng Li, Guanting Dong, Keming Lu, Chuanqi Tan, Chang Zhou, and Jingren Zhou. 2024. Scaling relationship on learning mathematical reasoning with large language models.	871
818		872
819		873
820		874
821	Zhiyuan Zeng, Qinyuan Cheng, Zhangyue Yin, Yunhua Zhou, and Xipeng Qiu. 2025. Revisiting the test-time scaling of o1-like models: Do they truly possess test-time scaling capabilities? <i>Preprint</i> , arXiv:2502.12215.	875
822		876
823		877
824		878
825		879
826	Lunjun Zhang, Arian Hosseini, Hritik Bansal, Mehran Kazemi, Aviral Kumar, and Rishabh Agarwal. 2024. Generative verifiers: Reward modeling as next-token prediction. In <i>The 4th Workshop on Mathematical Reasoning and AI at NeurIPS’24</i> .	880
827		881
828		882
829		883
830		884
831	Jialun Zhong, Wei Shen, Yanzeng Li, Songyang Gao, Hua Lu, Yicheng Chen, Yang Zhang, Wei Zhou, Jinjie Gu, and Lei Zou. 2025. A comprehensive survey of reward models: Taxonomy, applications, challenges, and future. <i>Preprint</i> , arXiv:2504.12328.	885
832		886
833		887
834		888
835		889
836	A Experimental Setup and Details	890
837	A.1 Main Experiment Setup	891
838	A.1.1 Policy Models and Reward Models	892
839	For our policy (generator) models, we evaluated a range of architectures and sizes to ensure comprehensive assessment of BEACON’s performance:	893
840		894
841		895
842	• LLaMA-3.2-3B-Instruct: Accessed and run locally on a GPU node equipped with 2 NVIDIA A100 GPUs.	896
843		897
844		898
845	• Qwen2.5-7B-Instruct: Inference conducted via DeepInfra’s API ¹ .	899
846		900
847	• Grok-3-Mini: Inference conducted via Grok’s API ² .	901
848		902
849	For our reward models (RMs), we utilized:	903
850	• NVIDIA Llama-3.1-Nemotron-70B-Reward: Accessed via NVIDIA’s API ³ services for response verification.	904
851		905
852		906
853	• Skywork-Llama-3.1-8B-Reward: Accessed and run locally on a GPU node equipped with 2 NVIDIA A100 GPUs.	907
854		908
855		909

¹<https://deepinfra.com/>

²<https://grok.x.ai/>

³https://build.nvidia.com/nvidia/llama-3_1-nemotron-70b-reward

856 A.1.2 Datasets and Evaluation Benchmarks

857 We evaluated BEACON on diverse reasoning and
858 alignment tasks:

859 **Reasoning Tasks:** The reasoning evaluation fo-
860 cused on mathematical problem-solving, reporting
861 average accuracy (Pass@1) across the following
862 benchmarks. For answer extraction and checking
863 mathematical equivalence, we utilized the expres-
864 sion matching tool from the Math-Verify reposi-
865 tory⁴ to ensure consistent and robust evaluation.

866

- 867 • **MATH500:** We used a randomly selected
868 subset of 50 problems from the MATH500
869 dataset (Hendrycks et al., 2021) to provide a
870 broad assessment without over-focusing on
871 this specific dataset, given its large size. The
872 problems are sampled from the test set.
- 873 • **AIME 2024:** All 30 problems from the Amer-
874 ican Invitational Mathematics Examination
875 2024 were used (Mathematical Association of
876 America, 2024)..
- 877 • **AMC 2023:** All 40 problems from the Amer-
878 ican Mathematics Competitions 2023 were
879 used, combining problems from AMC 10 and
880 AMC 12.

881 Alignment Task:

882

- 883 • **AlpacaEval 2.0:** We used the full set of 805
884 prompts from AlpacaEval 2.0 (Li et al., 2023).
885 The evaluation of response quality, comparing
886 model outputs against a reference (e.g., GPT-
887 4), was conducted using OpenAI’s API for
888 the automated evaluation protocol provided
889 by AlpacaEval. The primary metric reported
890 is the win rate.

891 A.1.3 Prompting Strategy

892 For all reasoning tasks, we employed a standard
893 one-shot Chain-of-Thought (CoT) prompting strat-
894 egy. The models were instructed to act as math as-
895 sistant and provide step-by-step solutions. Model-
896 specific instruction templates were used where ap-
897 propriate, but the core reasoning prompt structure
898 was as follows:

4⁴<https://github.com/huggingface/Math-Verify>

Standard CoT Reasoning Prompt

You are a math assistant. Solve problems step by step with clear reasoning.

Format:

1. Start with “Let me solve this step by step:”
2. Numbered steps with explanations
3. End with answer in box: 42

Rules:

- Answer must be integer or simplified fraction
- Use exact box format: 42
- No text after box
- For fractions: 3
4
- For negatives: -5

Example:

Let me solve this step by step:

1. First step
2. Second step
- ⋮
- N) Final step

42

[Problem Statement Here]

This standardized prompt ensures consistency in how tasks are presented to the policy models. For AlpacaEval, prompts are used as provided by the benchmark.

B Practical Guidelines for Setting the hyperparameters

The sampling cost parameter c plays a central role in BEACON, and should be viewed as the user’s tolerance towards both time and computational resources required for an additional sampling. As demonstrated in our main results, different values of c directly shape the optimization landscape of the value function $E[z_K - K \cdot c]$, with higher c

911 values consistently leading to earlier stopping on
912 average. Based on our comprehensive experiments
913 across multiple models and tasks, we recommend
914 setting $c = 0.1$ as an effective starting point, as
915 this value achieves significant sample reduction
916 (approximately 50-80% fewer samples than fixed
917 BoN) while preserving comparable accuracy for
918 both reward models across different task categories.
919 (highlight h-index table) to sample them in parallel
920 without constraint.

921 To determine the optimal c for specific deploy-
922 ment requirements, we recommend the following
923 calibration procedure:

- 924 **1. Establish performance baselines:** First,
925 run a small-scale experiment (e.g., 50-100
926 queries) using fixed BoN with a large sample
927 size (e.g., $N = 32$) to establish upper-bound
928 performance metrics (accuracy, reward).
- 929 **2. Sweep across c values:** Conduct a pa-
930 rameter sweep across a range of c values
931 (e.g., $c \in \{0.01, 0.05, 0.1, 0.2, 0.3, 0.4\}$) us-
932 ing BEACON on the same query set.
- 933 **3. Analyze the performance-efficiency Pareto
934 frontier:** For each c value, plot the resulting
935 performance metric (e.g., accuracy) versus av-
936 erage sample count \bar{K} . The optimal c lies at
937 the "knee point" of this curve where marginal
938 performance gains begin to diminish relative
939 to increased sampling costs.

940 In our experiments, we observed distinct patterns
941 across different model sizes and tasks:

- 942 • For smaller models (e.g., LLaMA-3.2-3B) on
943 reasoning tasks, $c \approx 0.1$ typically reduced
944 samples by $\sim 50\%$ while maintaining accuracy
945 within 1-2% of the full BoN baseline.
- 946 • For larger models (e.g., Grok-3-Mini) on
947 alignment tasks, $c \approx 0.3$ was often sufficient,
948 reducing samples by $\sim 85\%$ with minimal per-
949 formance degradation, as these models gen-
950 erally produced more consistent high-quality
951 responses. Note that to ensure fair compari-
952 son we still adapt same cost $c = 0.1$ for these
953 models.
- 954 • For time-sensitive applications (e.g., interac-
955 tive chatbots), higher values ($c \approx 0.2-0.3$)
956 prioritize responsiveness.

- 957 • For high-stakes applications (e.g., critical rea-
958 soning tasks), lower values ($c \approx 0.05$) favor
959 thoroughness.

960 The optimal value of c is inherently subjec-
961 tive, as some users may have stricter resource con-
962 straints or lower tolerance for computation time,
963 while others may prioritize response quality over
964 efficiency. In production environments, c can be
965 further contextualized to correspond to actual com-
966 putational costs.

967 Again we want to highlight that the key advan-
968 tage of BEACON is that regardless of how c is
969 set, our framework mathematically guarantees that
970 no resources are wasted through over-sampling or
971 under-sampling, given the specific resource con-
972 straint expressed through c . This adaptivity en-
973 sures BEACON consistently delivers the optimal
974 performance-efficiency trade-off aligned with the
975 user's particular tolerance for computational cost.
976 Furthermore, c can be dynamically adjusted based
977 on changing conditions, such as server load, time
978 of day, or query importance.

979 **B.1 Hyperparameter Selection Guide**

980 Based on the above analysis and guidandec, we
981 provide Table 3 which provides systematic guid-
982 ance for selecting optimal hyperparameters across
983 different application scenarios and model configu-
984 rations.

985 **B.2 Cost Parameter Calibration**

986 Table 4 demonstrates the systematic relationship
987 between cost parameter values and resulting perfor-
988 mance metrics, enabling data-driven hyperparame-
989 ter selection.

990 In practice, c can be calibrated to actual costs:
991 for API-based inference, set c proportional to $(\$/to-
992 ken) \times (\text{avg. tokens per sample})$; for self-hosted
993 deployment, $c \propto (\text{GPU hours}) \times (\text{hourly cost})$. For
994 instance, if generating one sample costs \$0.01 and
995 the reward scale is approximately $[-3, 3]$, setting
996 $c = 0.1$ implies stopping when the marginal ex-
997 pected gain falls below \$0.01.

998 **C Practical Implementation Details**

999 **C.1 Decoding Hyperparameters and 1000 BEACON Configuration**

1001 Besides cost, the BEACON framework operated
1002 with the following core settings for the main exper-
1003 iments:

Table 3: Hyperparameter Selection Guidelines

Application Type	Model Size (Params)	Optimal Cost (c)	Horizon (n)	Expected Samples (K)	Accuracy (%)	Primary Objective
Easy Reasoning	$\leq 7B$	0.15	16	4.2	85.1	Efficiency
Easy Reasoning	$\geq 70B$	0.30	16	3.1	87.4	Speed
Hard Reasoning	$\leq 7B$	0.05	32	12.8	52.9	Quality
Hard Reasoning	$\geq 70B$	0.10	32	8.4	58.2	Balanced
Creative Writing	$\leq 7B$	0.08	24	9.6	76.3	Diversity
Creative Writing	$\geq 70B$	0.20	16	5.2	82.1	Consistency
Code Generation	$\leq 7B$	0.06	32	14.1	68.7	Correctness
Code Generation	$\geq 70B$	0.12	24	7.8	75.4	Efficiency
Interactive Chat	Any	0.40	12	3.5	71.2	Latency
Batch Processing	Any	0.05	32	18.2	55.8	Thoroughness

Table 4: Cost Parameter Calibration Analysis

Cost (c)	Avg. Accuracy (%)	Avg. Samples (K)	Value Score $E[z_K - K \cdot c]$	95% Sample Count	Recommended Scenario
0.01	54.2	28.4	0.94	32.0	Research/Quality-critical
0.05	53.4	18.6	1.41	28.5	Hard reasoning tasks
0.10	52.9	12.8	1.61	22.1	Default (balanced)
0.20	51.8	8.2	1.54	16.4	General applications
0.30	50.1	5.9	1.33	12.8	Latency-sensitive
0.50	47.8	4.1	1.02	8.9	Interactive systems

Decoding Parameters: For all policy model inferences, unless specified otherwise by the API provider’s defaults for instructed models, we used consistent decoding parameters:

- Temperature: 0.7
- Maximum new tokens: 2048

BEACON Framework Configuration:

- Minimum initial samples (k_0): 3. This is required to properly establish the posterior Normal-Inverse-Gamma distribution using Jeffreys’ non-informative prior ($\mu_0 = 0, \nu_0 = 0, \alpha_0 = -0.5, \beta_0 = 0$).
- Maximum sampling horizon (T_{\max} or n): 32.
- H-index function $h_{n,k}(\hat{z}_k)$: Pre-computed based on the methodology in Baucells and Zorc (Baucells and Zorc, 2024) using the specified priors.

C.2 Iterative DPO with BEACON: Experimental Setup

C.2.1 Data Foundation for DPO Preference Generation

The prompts used for generating responses, which subsequently form preference pairs for Direct Preference Optimization (DPO), are drawn from the extensive training set of the MATH dataset (7,500 problems) (Hendrycks et al., 2021). The MATH dataset, comprising problems from American mathematics competitions like AMC 10, AMC 12, and AIME, is highly suitable due to its provision of full step-by-step solutions, which is beneficial for training models on complex derivations. Its effectiveness in enhancing mathematical reasoning is well-established. While preference data is generated from these MATH prompts, the DPO model’s performance is evaluated on the MATH500 benchmark, as presented in Figure 5 of the main text.

C.2.2 Fixed Reward Model for Ranking Responses

To rank the generated responses for constructing preference pairs (y_w, y_l) needed for DPO, similarly

1004
1005
1006
1007

1008

1009

1010

1011

1012

1013

1014

1015

1016

1017

1018

1019

1020

1021

1022

1023

1024

1025

1026

1027

1028

1029

1030

1031

1032

1033

1034

1035

1036

1037

1038

1040

1041

1042

1043

1044 to the main experiment, we use Skywork-llama3.1-
1045 8b as the base reward model. This reward model
1046 assigns a scalar score, denoted $R_{learned}$, to each
1047 policy-generated response, reflecting its assessed
1048 quality.

1049 **C.2.3 Preference Pair Generation Strategies 1050 for DPO**

1051 Preference pairs for each DPO iteration are gener-
1052 ated using one of two distinct strategies:

1053 **Best-of-N (BoN) Strategy.** For each prompt, a
1054 fixed $N = 16$ candidate responses are sampled
1055 from the current iteration of the policy model
1056 (Qwen2.5-7B-instruct). These N responses are
1057 then scored using the $R_{learned}$ value obtained from
1058 our reward model. The response with the highest
1059 $R_{learned}$ score is selected as the preferred response
1060 (y_w), and the response with the lowest $R_{learned}$
1061 score is chosen as the dispreferred response (y_l). If
1062 all 16 responses for a given prompt yield identical
1063 $R_{learned}$ scores, that prompt is excluded from the
1064 DPO training set for that iteration.

1065 **BEACON Strategy.** For each prompt, our BEA-
1066 CON algorithm is employed to adaptively deter-
1067 mine the number of samples K to generate. BEA-
1068 CON begins with an initial $k_0 = 3$ samples and
1069 can sample up to a maximum of $N_{max} = 16$ (es-
1070 pecially in early DPO iterations). As noted in the
1071 main text (Figure 5, right panel), the average K
1072 required by BEACON tends to decrease in later
1073 DPO iterations. BEACON utilizes an adapted re-
1074 ward signal, R_{BEACON} (the transformation from
1075 $R_{learned}$ is detailed in Appendix C.2.5), for both
1076 its internal Bayesian stopping decisions and for the
1077 final ranking of the K collected samples. From
1078 these K samples, the response yielding the high-
1079 est R_{BEACON} score is selected as y_w , and the one
1080 with the lowest R_{BEACON} score is selected as y_l .
1081 The same discard rule applies if all K responses
1082 result in identical R_{BEACON} scores.

1083 **C.2.4 Iterative Direct Preference 1084 Optimization Training**

1085 The policy model, Qwen2.5-7B-instruct, is fine-
1086 tuned using Direct Preference Optimization (DPO)
1087 (Rafailov et al., 2023) on the preference pairs
1088 (y_w, y_l) generated by either the BoN or BEACON
1089 strategy. Key hyperparameters for DPO training
1090 include a learning rate of 5×10^{-7} , a global batch
1091 size of 128, and a maximum sequence length of
1092 4096. In each DPO iteration, the policy model is

1093 trained for 2 epochs on the newly generated pref-
1094 erence dataset. The entire cycle of preference pair
1095 generation (using either BoN or BEACON) fol-
1096 lowed by DPO fine-tuning of the policy model is
1097 repeated for a total of 7 iterations.

1098 **C.2.5 Reward Adaptation for BEACON 1099 Algorithm**

1100 The BEACON algorithm, particularly its Bayesian
1101 parameter updates, expects a continuous reward
1102 signal to estimate the underlying reward distribu-
1103 tion effectively. While our foundational reward
1104 assessment might involve rule-based, binary out-
1105 comes (e.g., correct/incorrect), we adapt the score
1106 $R_{learned}$ from our fixed reward model (described in
1107 Appendix C.2.2) to better suit BEACON’s require-
1108 ments. This adaptation is based on the correctness
1109 of the final answer found within a $\boxed{\cdot}$ en-
1110 vironment in the generated response.

1111 Let $R_{learned}$ be the continuous score produced
1112 by our fixed reward model for a given response.
1113 The final reward, R_{BEACON} , used by the BEA-
1114 CON algorithm is determined as follows:

- 1115 • If the response contains the correct final an-
1116 swer in a $\boxed{\cdot}$ environment:
 - 1117 – If $R_{learned} > 0$, then $R_{BEACON} =$
1118 $R_{learned} \times 2$.
 - 1119 – If $R_{learned} \leq 0$, then $R_{BEACON} =$
1120 $R_{learned}/2$ (making a non-positive score
1121 less detrimental if the final answer is sur-
1122 prisingly correct).
- 1123 • If the response contains an incorrect final an-
1124 swer in a $\boxed{\cdot}$ environment:
 - 1125 – If $R_{learned} > 0$, then $R_{BEACON} =$
1126 $R_{learned}/2$ (penalizing a score that
1127 might have seemed good otherwise).
 - 1128 – If $R_{learned} \leq 0$, then $R_{BEACON} =$
1129 $R_{learned} \times 2$ (further penalizing an al-
1130 ready non-positive score).
- 1131 • If the response fails to provide any final an-
1132 swer in a $\boxed{\cdot}$ environment, the
1133 reward remains unchanged: $R_{BEACON} =$
1134 $R_{learned}$.

1135 **D Additional Theoretical Analysis and 1136 Proofs**

1137 This section provides supplementary theoretical
1138 background and proofs for the BEACON frame-
1139 work.

D.1 Classical Sequential Search Problem

In the classical sequential search problem (Weitzman, 1979), a decision maker (DM) faces an infinite sequence of independent offers $\{x_1, x_2, \dots\}$ drawn from a known distribution function F with density f . Sampling incurs a constant cost $c > 0$, and the DM may stop at any time, accepting the highest offer observed so far (see Figure 6 for illustration). Since the distribution F is fully known, the predictive distribution remains unchanged throughout the process.

The dynamic programming recursion for the value function after k samples is:

$$V(z) = \max \left\{ z, \int_{-\infty}^{\infty} V(\max\{z, y\}) dF(y) - c \right\}$$

where z is the current best observed offer. The associated gain from one more search is $H(z) = \int_z^\infty (y - z) dF(y)$, representing the expected improvement conditional on continuing.

A fundamental property is the **reservation price property**: there exists a threshold r^* such that the optimal policy is to stop if and only if $z \geq r^*$. This reservation price solves:

$$c = H(r^*) = \int_{r^*}^{\infty} (y - r^*) dF(y).$$

The DM thus compares the sampling cost with the expected marginal benefit; once the best offer reaches r^* , the expected gain no longer justifies continued search.

This threshold-based policy has important implications: (1) r^* depends only on F and c , not on the number of samples or their sequence; (2) as c increases, r^* decreases, leading to earlier stopping; and (3) distributions with heavier right tails yield higher reservation prices, reflecting greater potential benefits from continued search.

D.2 Priors and Minimal Sample Size for Bayesian Updating

We employ a conjugate Normal-Inverse-Gamma prior for the unknown mean μ and variance σ^2 of the reward distribution, following (Baucells and Zorc, 2024). In this framework, the precision $1/\sigma^2$ follows a Gamma distribution with parameters (α_0, β_0) , and conditional on precision, μ follows a Normal distribution with mean μ_0 and variance σ^2/ν_0 . This structure enables analytical posterior updates with hyperparameters $(\alpha_k, \nu_k, \beta_k, \mu_k)$. Starting with prior $\text{NIG}(\mu_0, \nu_0, \alpha_0, \beta_0)$ and after

observing k samples, the posterior parameters become:

$$\begin{aligned}\alpha_k &= \alpha_0 + \frac{k}{2}, \nu_k = \nu_0 + k, \mu_k = \frac{\nu_0 \mu_0 + k \bar{r}_k}{\nu_0 + k}, \\ \beta_k &= \beta_0 + \frac{\sum_{i=1}^k (r_i - \bar{r}_k)^2}{2} + \frac{k \nu_0 (\bar{r}_k - \mu_0)^2}{2(\nu_0 + k)},\end{aligned}\tag{4}$$

where \bar{r}_k is the sample mean. The posterior predictive distribution follows a Student-t distribution with $2\alpha_k$ degrees of freedom, mean μ_k , and scale parameter $\sigma_k = \sqrt{(\nu_k + 1)\beta_k}/(\nu_k\alpha_k)$.

Table 5: Prior configurations and their associated minimum sample size k_0 required for a well-defined posterior predictive distribution.

Prior Configuration	k_0
$2\alpha_0 > 1, \nu_0, \beta_0 > 0$	0
$2\alpha_0 \in (0, 1], \nu_0 > 0, \beta_0 \geq 0$	1
$2\alpha_0 > 1, \nu_0 > 0, \beta_0 = 0$	1
$\alpha_0, \beta_0 > 0, \nu_0 = 0$	1
$\alpha_0 > 0, \nu_0 = \beta_0 = 0$	2
$2\alpha_0 \in (-1, 0], \nu_0, \beta_0 \geq 0$	2
$2\alpha_0 = -1, \nu_0, \beta_0 \geq 0$	3

The minimal sample size k_0 depends on the chosen prior hyperparameters. For BEACON, we adopt Jeffreys' non-informative prior $(\alpha_0, \nu_0, \beta_0) = (-1/2, 0, 0)$, which requires $k_0 = 3$ initial observations before a valid posterior predictive distribution emerges. More informative priors require fewer initial samples, as summarized in Table 5.

D.3 Sufficient Statistics for the Search Problem using Bayesian Updating

The Bayesian sequential search model can be significantly simplified through sufficient statistics that encapsulate all relevant information for optimal stopping decisions (Baucells and Zorc, 2024).

Lemma 1. For any sampling stage k , where $k_0 \leq k \leq n$, the triple (z_k, μ_k, σ_k) together with k constitute sufficient statistics for the value-to-go function $V_{n,k}(\mathbf{r}_k; c)$.

This lemma establishes that rather than tracking the complete observation history $r_k = \{r_1, \dots, r_k\}$, we only need to maintain three key statistics:

- $z_k = \max\{r_1, \dots, r_k\}$: The highest observed reward so far
- μ_k : The posterior mean of the reward distribution

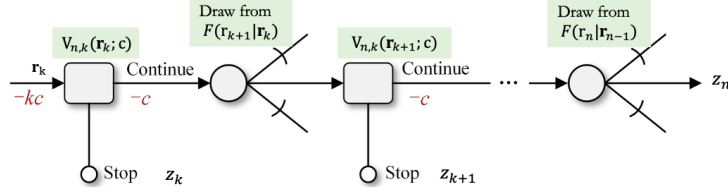


Figure 6: Sequential search problem illustration: At each step, the decision-maker observes a reward r_k and decides whether to stop with the current best reward z_k or continue sampling, incurring cost c .

- σ_k : The scale parameter derived from the posterior distribution

These statistics update efficiently according to the following formula when observing a new reward r_{k+1} :

$$z_{k+1} = \max\{z_k, r_{k+1}\}, \quad (5)$$

$$\mu_{k+1} = \mu_k + \frac{r_{k+1} - \mu_k}{\nu_0 + k + 1}, \quad (6)$$

$$\sigma_{k+1} = \sqrt{\frac{1 - \frac{1}{(\nu_0 + k + 1)^2}}{2\alpha_0 + k + 1}} \times \sqrt{(2\alpha_0 + k)\sigma_k^2 + (r_{k+1} - \mu_k)^2}. \quad (7)$$

The posterior predictive distribution follows a Student-t distribution with $2\alpha_k$ degrees of freedom. This statistical sufficiency substantially simplifies both theoretical analysis and practical implementation of BEACON by reducing the problem's dimensionality from tracking k individual rewards to monitoring just three informative statistics, making the algorithm computationally efficient and mathematically tractable.

D.4 Details of Universal Index Policy

Here we elaborate on the Universal Index Policy.

Definition 2. For $k_0 \leq k < n$, the index function $h_{n,k} : \mathbb{R} \rightarrow (0, \infty)$ maps each standardized best reward $\hat{z} \in \mathbb{R}$ to the unique value $c > 0$ that solves $H_{n,k}(\hat{z}, 0, 1; c) = c$.

This definition captures how the h-index represents the exact cost threshold where the expected value of continuing equals that of stopping. The strength of this approach is its reusability—once computed, these indices apply across different queries with similar statistical properties.

Theorem 2. (Baucells and Zorc, 2024) After $k \geq k_0$ observations, with standardized best reward $\hat{z}_k = (z_k - \mu_k)/\sigma_k$, it is optimal to stop and accept z_k if $c \geq \sigma_k h_{n,k}(\hat{z}_k)$, and continue searching otherwise. Equivalently, stop if and only if $\hat{z}_k \geq h_{n,k}^{-1}(c/\sigma_k)$.

Theorem 3. (Baucells and Zorc, 2024) The h-index function $h_{n,k}(\hat{z})$ for $k_0 \leq k < n$ is strictly decreasing, convex, and satisfies $\lim_{\hat{z} \rightarrow \infty} h_{n,k}(\hat{z}) = 0$.

This theorem establishes BEACON's core stopping criterion—after normalizing the current best reward, we stop sampling when the cost-adjusted index threshold is reached. This occurs when the current best reward is sufficiently high relative to our uncertainty about the reward distribution, considering the sampling cost.

D.5 Computation of the h-index

Computing the h-index function $h_{n,k}(\hat{z})$ requires solving recursive equations based on the Bellman equation and expected marginal gain function $H_{n,k}$ from §2.2. As derived in (Baucells and Zorc, 2024), we need to solve:

$$H_{n,k}(\hat{z}, 0, 1; c) = H_{k+1,k}(\hat{z}, 0, 1; c) + \int \sigma_u \cdot g(u) dF_{2\alpha}(u), \quad (8)$$

where

$$g(u) = \max \left\{ 0, H_{n,k+1} \left(\frac{z_u - \mu_u}{\sigma_u}, 0, 1; \frac{c}{\sigma_u} \right) \right\}$$

with boundary condition $H_{n,n} = 0$, where $z_u = \max\{\hat{z}, u\}$, $\mu_u = u/(\nu_0 + k + 1)$, $\sigma_u = \Lambda_{k+1} \sqrt{2\alpha_0 + k + u^2}$, $\Lambda_{k+1} = \sqrt{\frac{2\alpha_0 + k}{2\alpha_0 + k + 1}}$, and $F_{2\alpha}$ is the CDF of the Student-t distribution with $2\alpha_0$ degrees of freedom.

In our implementation, we pre-compute the h-index function $h_{n,k}(\hat{z})$ for each time horizon n using Jeffreys' non-informative prior ($\alpha_0 = -0.5, \nu_0 = 0$). We create a lookup table using a geometric grid of $\hat{z}_k \in [-30, 30]$ with resolution $G = 100$ for all timesteps $k \in [3, n]$, leveraging an optimized implementation⁵ with Numba for parallel processing.

⁵<https://github.com/MSORlearners/h-index-computation.git>

1286 During inference, BEACON evaluates the stop-
 1287 ping condition through constant-time linear inter-
 1288 polation on this pre-computed table, enabling effi-
 1289 cient decision-making during sequential sampling
 1290 without the computational overhead of dynamic
 1291 programming calculations at runtime.

1292 D.6 Binary-Reward Variant: Bernoulli-Beta 1293 Learning

1294 **Model.** Consider the sequential generation pro-
 1295 cess in Section 2.2 with binary rewards $r_i \in \{0, 1\}$
 1296 and unknown success probability $\theta \in (0, 1)$. Con-
 1297 ditional on θ , the draws are i.i.d. $\text{Bernoulli}(\theta)$.
 1298 Sampling incurs a per-draw cost $c > 0$ and the hori-
 1299 zon is at most n draws. Let $\mathbf{r}_k = (r_1, \dots, r_k)$ and
 1300 $z_k = \max\{r_1, \dots, r_k\} \in \{0, 1\}$ be the best ob-
 1301 served reward by stage k . Adopt the conjugate prior
 1302 $\theta \sim \text{Beta}(a_0, b_0)$ with $a_0, b_0 > 0$. After k draws
 1303 with $s_k = \sum_{i=1}^k r_i$ successes and $f_k = k - s_k$
 1304 failures, the posterior is

$$1305 \theta \mid \mathbf{r}_k \sim \text{Beta}(a_k, b_k), \quad a_k = a_0 + s_k, \quad b_k = b_0 + f_k,$$

1306 and the posterior-predictive probability of success
 1307 on the next draw is

$$1308 q_k = \Pr(r_{k+1} = 1 \mid \mathbf{r}_k) = a_k / (a_k + b_k).$$

1309 The sufficient statistics are (z_k, a_k, b_k) . Upon ob-
 1310 serving r_{k+1} ,

$$1311 z_{k+1} = \max\{z_k, r_{k+1}\}, \quad (9)$$

$$1312 a_{k+1} = a_k + r_{k+1}, \quad b_{k+1} = b_k + 1 - r_{k+1}. \quad (10)$$

1313 **Dynamic program.** If $z_k = 1$ the process is ab-
 1314 sorbing and the decision maker stops with value
 1315 1. When $z_k = 0$, let $V_{n,k}(0, a_k, b_k; c)$ denote the
 1316 optimal value (with at most n draws total, at stage
 1317 k). Then

$$1318 V_{n,k}(0, a_k, b_k; c) = \max\{0, v_k(c)\}, \quad (11)$$

$$1319 V_{n,n}(0, a_n, b_n; c) = 0, \quad V_{n,k}(1, a_k, b_k; c) = 1, \quad (12)$$

1320 where $v_k(c) = q_k + (1 - q_k) V_{n,k+1}(0, a_k, b_k +
 1321 1; c) - c$, and $q_k = a_k / (a_k + b_k)$.

1322 It is convenient to rewrite the recursion in
 1323 remaining-draws form. Let $R_t(a, b; c)$ be the op-
 1324 timal value with $t \in \{0, 1, \dots\}$ draws remaining
 1325 and no success yet. With $R_0(\cdot) \equiv 0$,

$$1326 R_t(a, b; c) = \max\{0, q(a, b) +
 1327 (1 - q(a, b)) R_{t-1}(a, b + 1; c) - c\}, \quad (13)$$

1328 where $q(a, b) = a / (a + b)$. The connection to (11)
 1329 is $V_{n,k}(0, a_k, b_k; c) = R_{n-k}(a_k, b_k; c)$.

1329 **Reservation cost and optimal policy.** For each
 1330 stage, there is a unique cost threshold at which the
 1331 decision maker is indifferent between stopping and
 1332 taking one more draw.

1333 **Lemma 2** (Basic properties of R_t). *For fixed
 1334 (t, a, b) with $t \geq 1$ and $a, b > 0$, the map $c \mapsto
 1335 R_t(a, b; c)$ is continuous, nonincreasing, and 1-
 1336 Lipschitz on $[0, \infty)$. Moreover $R_t(a, b; 0) > 0$
 1337 and $R_t(a, b; 1) = 0$; hence $\{c > 0 : R_t(a, b; c) >
 1338 0\} \subset (0, 1)$.*

1339 **Proof:** Induct on t . The base $t = 0$ is trivial
 1340 since $R_0 \equiv 0$. Suppose the claim holds for $t - 1$.
 1341 The inner term

$$\psi_t(c) := q(a, b) + (1 - q(a, b)) R_{t-1}(a, b + 1; c) - c \quad (1342)$$

1343 is continuous and 1-Lipschitz as a sum of a con-
 1344 stant, a nonnegative multiple of a 1-Lipschitz func-
 1345 tion, and $-c$. The outer map $x \mapsto \max\{0, x\}$
 1346 is continuous and 1-Lipschitz, hence so is $R_t =
 1347 \max\{0, \psi_t\}$. Monotonicity in c follows from the
 1348 $-c$ term. For $c = 0$, $R_t(a, b; 0) \geq R_1(a, b; 0) =
 1349 q(a, b) > 0$. For $c = 1$, since $R_{t-1}(a, b + 1; 1) \leq
 1350 R_{t-1}(a, b + 1; 0)$ and $q(a, b) \leq 1$, one has $\psi_t(1) \leq
 1351 q(a, b) - 1 \leq 0$, hence $R_t(a, b; 1) = 0$. \square

1352 **Lemma 3** (Strictly decreasing “continue” margin).
 1353 Define $\phi_t(c) := q(a, b) + (1 - q(a, b)) R_{t-1}(a, b +
 1354 1; c) - c$. Then ϕ_t is continuous and strictly de-
 1355 creasing on $[0, \infty)$, with $\phi_t(0) > 0$ and $\phi_t(1) \leq 0$.

1356 **Proof:** Continuity follows from Lemma 2. If
 1357 $0 \leq c_0 < c_1$, then using that R_{t-1} is nonincreasing
 1358 and 1-Lipschitz,

$$\phi_t(c_1) - \phi_t(c_0) = (1 - q)(R_{t-1}(c_1) - R_{t-1}(c_0))
 1359 - (c_1 - c_0) \leq 0 - (c_1 - c_0) < 0, \quad (1360)$$

1361 so ϕ_t is strictly decreasing. The sign claims are
 1362 from Lemma 2. \square

1363 **Theorem 4** (Reservation-cost policy). *Fix n
 1364 and a stage $k < n$ with posterior parameters
 1365 (a_k, b_k) . There exists a unique reservation cost
 1366 $h_{n,k}^B(a_k, b_k) \in [0, 1]$ such that*

$$V_{n,k}(0, a_k, b_k; c) > 0 \iff c < h_{n,k}^B(a_k, b_k). \quad (1367)$$

1368 Equivalently, $h_{n,k}^B(a_k, b_k)$ is the unique solution c
 1369 to

$$c = \frac{a_k}{a_k + b_k} + \frac{b_k}{a_k + b_k} V_{n,k+1}(0, a_k, b_k + 1; c). \quad (14) \quad (1370)$$

1371 The Bayes-optimal policy is: if $z_k = 1$, stop and
 1372 obtain 1; if $z_k = 0$, continue iff $c < h_{n,k}^B(a_k, b_k)$.

1373 **Proof:** Work with R_t at $t = n - k$. By
 1374 Lemma 3, ϕ_t is strictly decreasing and continuous
 1375 with $\phi_t(0) > 0$ and $\phi_t(1) \leq 0$, hence it
 1376 has a unique root $h_t(a, b) \in [0, 1]$. From (13),
 1377 $R_t = \max\{0, \phi_t\}$, so $R_t > 0$ iff $c < h_t(a, b)$.
 1378 Continuity gives $\phi_t(h_t) = 0$, which is (14) after
 1379 mapping (t, a, b) back to (n, k, a_k, b_k) . The stated
 1380 action rule is exactly the comparison between the
 1381 two branches in (11), while $z_k = 1$ is absorbing
 1382 with value 1. \square

1383 **BEACON:** For binary rewards, BEACON replaces
 1384 the continuous Normal framework with Bernoulli-
 1385 Beta conjugate learning. The stopping criterion
 1386 from Theorem 1 becomes the binary reservation
 1387 cost policy in Theorem 4, while the sufficient statistics
 1388 (5) are replaced with the simpler Beta updates
 1389 (9). This maintains BEACON’s sequential structure
 1390 while using binary-specific optimal stopping decisions.

1392 D.7 Proof of Theorem 1

1393 **Proof.** Under the Normal reward model with
 1394 Normal–Inverse–Gamma prior, (z_k, μ_k, σ_k) (to-
 1395 gether with k) are sufficient statistics for the state
 1396 (Lemma in Appendix D.3). Standardizing gives
 1397 $\hat{z}_k = (z_k - \mu_k)/\sigma_k$ and reduces the problem to the
 1398 canonical (location–scale normalized) sequential
 1399 search instance.

1400 By Theorem 2 (Universal Index Policy), for the
 1401 canonical problem there exists a strictly decreasing
 1402 index function $h_{n,k}(\cdot)$ such that the (myopic)
 1403 continuation rule

$$1404 \text{Continue at step } k \iff h_{n,k}(\hat{z}_k) > \frac{c}{\sigma_k}$$

1405 maximizes the Bellman value function. Translating
 1406 back to original (unscaled) variables yields exactly
 1407 condition (3). Therefore the stopping time

$$1408 K = \min\{k \geq k_0 : h_{n,k}(\hat{z}_k) \leq c/\sigma_k\} \wedge n$$

1409 achieves the optimal value $\mathbb{E}[z_K - Kc]$.

1410 Optimality of K follows because: (i) any earlier
 1411 stop with $h_{n,k}(\hat{z}_k) > c/\sigma_k$ forgoes strictly positive
 1412 expected marginal gain; (ii) any continuation with
 1413 $h_{n,k}(\hat{z}_k) \leq c/\sigma_k$ incurs cost exceeding expected
 1414 benefit; (iii) strict monotonicity of $h_{n,k}$ implies
 1415 no alternative rule can dominate. Hence K is the
 1416 unique optimal stopping time under the stated as-
 1417 sumptions. \square

1418 D.8 Sensitivity Analysis

1419 **Proposition 1.** *The optimal stopping time K under
 1420 the policy is influenced by several factors: it de-*

creases with higher sampling cost c and larger current best reward z_k , while increasing with higher posterior mean μ_k and greater posterior scale parameter σ_k . Additionally, the algorithm becomes more patient (tend to continue) when more remaining samples ($n - k$) are available.

1421 **Proof of Proposition 1 Proof:** From Theorem
 1422 3, we know that the h-index function $h_{n,k}(\hat{z})$ for
 1423 $k_0 \leq k < n$ is strictly decreasing, convex, and
 1424 satisfies $\lim_{\hat{z} \rightarrow \infty} h_{n,k}(\hat{z}) = 0$.

1425 Under the UIP stopping criterion in Equation
 1426 (3), stopping occurs when $h_{n,k}(\hat{z}_k) \leq \frac{c}{\sigma_k}$. Since
 1427 $h_{n,k}(\hat{z})$ is strictly decreasing, higher c raises the
 1428 threshold $h_{n,k}^{-1}(c/\sigma_k)$, leading to earlier stopping
 1429 (smaller K).

1430 For a fixed standardized best reward \hat{z} , the h-
 1431 index function $h_{n,k}(\hat{z})$ is increasing in $n - k$ (the
 1432 number of remaining samples) as shown in Bau-
 1433 cells and Zorc (2024). This means that when more
 1434 samples remain available (larger $n - k$), the thresh-
 1435 old for stopping becomes higher, making the algo-
 1436 rithm more "patient" and likely to continue sam-
 1437 pling.

1438 With $\hat{z}_k = \frac{z_k - \mu_k}{\sigma_k}$, higher z_k increases \hat{z}_k , which
 1439 decreases $h_{n,k}(\hat{z}_k)$ due to the function’s monotonic-
 1440 ity, resulting in earlier stopping. Conversely, higher
 1441 μ_k decreases \hat{z}_k , thereby increasing $h_{n,k}(\hat{z}_k)$ and
 1442 extending sampling (larger K). The scale parame-
 1443 ter σ_k affects stopping through dual mechanisms:
 1444 it decreases \hat{z}_k by appearing in the denominator
 1445 and simultaneously decreases $\frac{c}{\sigma_k}$. Both effects in-
 1446 crease $h_{n,k}(\hat{z}_k)$ relative to $\frac{c}{\sigma_k}$, encouraging contin-
 1447 ued sampling (larger K).

1448 E Additional Experimental Results

1449 E.1 Statistical Significance Analysis of 1450 BEACON

1451 To assess the reliability of our results, we present
 1452 a focused analysis using LLaMA-3.2-3B as our
 1453 base model. Each experiment was conducted with
 1454 5 different random seeds, and we report the error
 1455 bars as the standard error of the mean (SEM). As
 1456 shown in Table 6, BEACON achieves comparable
 1457 performance to the BoN baseline in terms of accu-
 1458 racy ($32.8 \pm 1.6\%$ vs. $33.4 \pm 1.3\%$ for reasoning
 1459 tasks) and win rate ($23.5 \pm 1.8\%$ vs. $25.0 \pm 2.5\%$ for
 1460 alignment tasks), with overlapping error margins
 1461 indicating no substantial performance degradation.
 1462 However, BEACON requires significantly fewer
 1463 samples (15.8 ± 1.2 vs. 32.0 for reasoning tasks),
 1464 resulting in substantially higher value scores that

Table 6: Comparison of BEACON with baseline methods using LLaMA-3.2-3B. Results shown as mean \pm SEM across 5 random seeds.

Method	Reasoning Tasks (Avg. MATH/AIME/AMC)				Alignment Task (AlpacaEval 2.0)			
	Acc. \uparrow (%)	Samples \downarrow (\bar{K})	Reward \uparrow (Scaled)	Value \uparrow (Scaled)	Win \uparrow (%)	Samples \downarrow (\bar{K})	Reward \uparrow (Scaled)	Value \uparrow (Scaled)
Direct CoT	20.0 \pm 2.8	1.0	-1.60 \pm 0.10	-0.40 \pm 0.05	16.0 \pm 3.5	1.0	0.20 \pm 0.05	-0.80 \pm 0.08
BoN (N-RM)	33.4 \pm 1.3	32.0	3.49 \pm 0.22	0.29 \pm 0.14	25.0 \pm 2.5	32.0	4.00 \pm 0.25	0.80 \pm 0.09
BEACON (N-RM)	32.8 \pm 1.6	15.8 \pm 1.2	3.25 \pm 0.18	1.12 \pm 0.21	23.5 \pm 1.8	14.5 \pm 2.3	3.65 \pm 0.22	1.20 \pm 0.20

account for both performance and computational cost (1.12 \pm 0.21 vs. 0.29 \pm 0.14).

E.2 Impacts of Cost on the Value Optimizations

The sampling cost, denoted by c , plays a critical role in the optimization of our value function, which serves as the core objective for determining the optimal stopping criterion. As illustrated in Figure 3, variations in the cost parameter directly influence the shape and peak of the value function and the resulting optimal sample size. The left subplot of Figure 3 shows that for any given sampling cost, the value function initially increases with the number of samples as the expected reward grows when we have more sample option to select, but eventually decreases as the cumulative cost outweighs the marginal gain from additional samples. Notably, increasing the sampling cost leads to a lower maximum achievable value and shifts the point of optimal stopping (where the value function peaks) towards a smaller number of samples. The right subplot of Figure 3 further emphasizes this relationship by directly plotting the optimal sample size against the sampling cost. This plot clearly demonstrates a strong inverse correlation: as the cost of obtaining each sample increases, the BEACON framework optimally decides to stop sampling earlier, resulting in a significantly reduced optimal sample size.

E.3 Normality Analysis of Reward Distributions

While BEACON leverage learning for reward estimation, we acknowledge that real-world reward distributions from LLMs may not always strictly adhere to normality. This appendix section visually explores the characteristics of reward distributions observed in our experiments using the Nemotron reward model, providing context for our robust updating mechanism.

Figure 7 presents an aggregated view of reward distributions, conditioned on whether the generated responses were ultimately deemed correct or incorrect. We observe that for both categories, the empirical distributions of rewards are reasonably approximated by a normal distribution, albeit with different means and variances. Specifically, correct answers tend to receive higher mean rewards, but both distributions exhibit a unimodal, bell-like shape characteristic of normality. This overall trend provides a foundational justification for employing a Gaussian-based learning model.

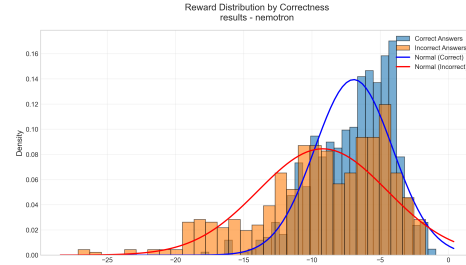


Figure 7: Aggregated reward distributions from the Nemotron RM, separated for responses classified as correct (blue histogram, blue normal fit) and incorrect (orange histogram, red normal fit). Both distributions show approximate normality.

However, analyzing distributions at an aggregate level can mask variations in individual query-specific reward patterns. Therefore, Figure 8 dives into specific cases to illustrate the types of reward distributions encountered for individual prompts. The leftmost panel ("Normal Question 8") depicts a common scenario where the rewards for multiple samples from a single prompt follow an approximately normal distribution, though the specific mean and variance naturally differ from prompt to prompt. In contrast, the middle panel ("Non-Normal Question 3") illustrates an occasional but important pattern: the distribution consists primarily of high-reward samples with a few significantly

lower, noisy rewards in the left tail. This type of skewed distribution, or one with outliers, can badly influence standard posterior parameter updates. But it is precisely these instances that motivate BEACON’s robust updating formula, which is designed to mitigate the impact of such extreme low-value outliers, thereby maintaining a more stable and reliable estimation of the reward potential focused on the right tail. The rightmost panel ("All Questions") shows the overall distribution of all rewards for context.

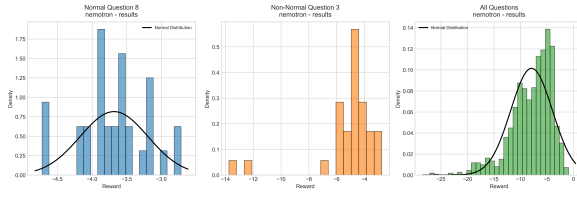


Figure 8: Examples of query-specific reward distributions using the Nemotron RM. Left: A typical case exhibiting approximate normality ("Normal Question 8"). Middle: An occasional case with predominantly high rewards and some low-value outliers ("Non-Normal Question 3"), motivating robust updates. Right: Aggregate distribution of all rewards.

These observations support our approach: while normality is a useful working assumption for the bulk of reward behaviors, the adaptive robust update mechanism provides resilience against deviations, particularly those caused by uninformative low scores, ensuring BEACON remains effective across diverse and sometimes non-ideal reward landscapes.

E.4 Robust Updating Formula and Details

Robust Update Rule. To mitigate negative skewness and extreme left-tail outliers, we modify the standard posterior update by filtering rewards below the 1% posterior-predictive quantile. Specifically,

$$z_{k+1} = \max\{z_k, r_{k+1}\}, \quad (15)$$

$$\tilde{r}_{k+1} = \begin{cases} \mu_k, & \text{if } r_{k+1} < q_{0.01}, \\ r_{k+1}, & \text{otherwise,} \end{cases} \quad (16)$$

$$\mu_{k+1} = \mu_k + \frac{\tilde{r}_{k+1} - \mu_k}{\nu_0 + k + 1}, \quad (17)$$

$$\sigma_{k+1} = \sqrt{\frac{1 - \frac{1}{(\nu_0 + k + 1)^2}}{2\alpha_0 + k + 1} \times \sqrt{(2\alpha_0 + k)\sigma_k^2 + (\tilde{r}_{k+1} - \mu_k)^2}}. \quad (18)$$

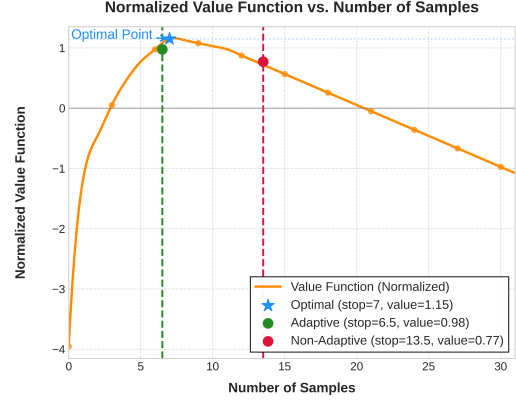


Figure 9: Value Estimation for the robust parameter update method (adaptive) vs. non-adaptive method. Our design helps BEACON avoid violating assumptions and stop closer to the optimum on average.

where $q_{0.01} = F_{2\alpha_k}^{-1}(0.01 \mid \mu_k, \sigma_k)$ is the 1% quantile of the posterior predictive distribution.

Interpretation. This one-sided winsorization caps the influence of extreme left-tail samples at the posterior mean, reducing variance inflation while leaving the maximum statistic z_{k+1} intact unless a new best reward is observed. The adjustment preserves the right-tail fidelity of the reward distribution, which is essential for correctly identifying high-quality responses.

Practical Notes. (i) The choice of threshold p is robust across $[0.5\%, 2\%]$, with $p = 1\%$ as default. (ii) The update is $O(1)$ per step; quantiles can be pre-tabulated for efficiency. (iii) For numerical stability, enforce $\sigma_k \geq 10^{-6}$. (iv) Optionally, robust updates can be activated only when recent empirical skewness is strongly negative (e.g., $\gamma_1 < -0.5$).

Results.

E.5 Case Analysis: Solution Diversity and Failure Analysis

The BEACON framework employs an adaptive stopping mechanism that dynamically adjusts the number of samples (K) based on the expected marginal gain from additional sampling, relative to the sampling cost c and posterior uncertainty about the reward distribution (σ_k). This mechanism inherently influences the diversity of generated solution candidates, balancing exploration breadth with computational efficiency. The stopping decision is driven by the consistency of reward model (RM) scores (reflected in σ_k), the quality of the current best response (z_k relative to μ_k), and the

Table 7: Examples of BEACON Behavior and Sample Diversity

Scenario Type	Example Prompt	S1 (Out & z_k)	S2 (Out & z_k)	S3 (Out & z_k)	S4 (Out & z_k)	S5 (Out & z_k)	S6 (Out & z_k)	Stops (K)	Diversity
Easy / High Reward	What is $2 + 2$?	Equals 4. ($z_k \approx 0.95$)	The sum is 4. ($z_k \approx 0.98$)	2+2 is 4. ($z_k \approx 0.96$)				Early ($K = 3$)	Low
Hard / Low Reward	Simple proof of Fermat’s Last Theorem...	[Failed Proof 1] ($z_k \approx -2.0$)	[Failed Proof 2] ($z_k \approx -2.2$)	[Failed Proof 3] ($z_k \approx -1.8$)				Early ($K = 3$)	Low
Moderately Hard / Improving	Simplify $\sqrt{242}$	Incorrect: $2\sqrt{60.5}$ ($z_k \approx -1.5$)	Error: $\sqrt{200} + \sqrt{42}$ ($z_k \approx -1.2$)	Correct: $11\sqrt{2}$ ($z_k \approx 0.95$)	Correct: $11 \cdot \sqrt{2}$ ($z_k \approx 0.93$)	Correct: $\sqrt{121 \cdot 2} = 11\sqrt{2}$ ($z_k \approx 0.96$)		Moderate ($K = 5$)	Medium
Very Hard / Inconsistent	How did US states get their names?	Brief: “Native words, kings.” ($z_k \approx 0.1$)	Partial: “VA from Virgin Queen...” ($z_k \approx 0.3$)	Flawed: “All named after presidents.” ($z_k \approx -0.5$)	Better: “Native Am. languages...” ($z_k \approx 0.8$)	Comprehensive		Late ($K \geq 5$)	High
High Patience / Extended	Outline three approaches to climate change.	Approach A ($z_k \approx 0.6$)	Approach B ($z_k \approx 0.5$)	Approach A (detailed) ($z_k \approx 0.85$)	Approach B (detailed) ($z_k \approx 0.88$)	Approach C (detailed) ($z_k \approx 0.90$)	Approach D ($z_k \approx 0.92$)	Late ($K \geq 6$)	High

Note: S_i denotes Sample i . z_k values are illustrative, based on Nemotron RM scores.

remaining sample budget ($n - k$), as governed by the Universal Index Policy (UIP).

Table 7 illustrates BEACON’s behavior across diverse scenarios, highlighting how these factors affect stopping time and sample diversity. The examples are drawn from empirical observations on benchmarks like MATH500 and AlpacaEval 2.0, with quantitative insights into failure modes.

- Easy Queries with Consistent High Rewards:** For simple queries (e.g., Example 1: “What is $2 + 2$?”), initial samples $\{y_k\}_{k=1}^{k_0}$ yield uniformly high RM scores ($z_k \approx 0.95$, low σ_k). Low posterior variance indicates that further sampling is unlikely to improve the best response, leading BEACON to stop early ($K = 3$). This results in low sample diversity, as responses are similar and high-quality. In our experiments, approximately 20% of MATH500 queries exhibited this behavior, stopping at $K \leq 3$ with $\sigma_k < 0.1$.
- Hard Queries with Consistent Low Rewards:** For extremely difficult queries (e.g., Example 2: “Simple proof of Fermat’s Last Theorem...”), samples consistently receive low RM scores ($z_k \approx -2.0$, low σ_k). BEACON terminates early ($K = 3$) due to low expected marginal gain, yielding low diversity. About 25% of AIME24 queries showed this pattern, with early stopping when $\mu_k < -1.5$. A failure mode occurs if the RM underestimates a potentially correct response, leading to premature stopping (observed in 2% of cases).

• Moderately Hard Queries with Improving Rewards:

For queries of moderate difficulty (e.g., Example 3: “Simplify $\sqrt{242}$ ”), initial samples may be incorrect ($z_k \approx -1.5$), but subsequent samples improve ($z_k \approx 0.95$). BEACON continues sampling to reduce σ_k and confirm consistency, stopping at moderate K (e.g., $K = 5$). This produces medium diversity, with varied incorrect and correct responses. In MATH500, 40% of queries followed this pattern, with $K = 4 - 6$. A failure mode arises if early incorrect samples inflate σ_k , delaying stopping (observed in 5% of cases).

• Very Hard or Ambiguous Queries with Inconsistent Rewards:

For complex or ambiguous queries (e.g., Example 4: “How did US states get their names?”), RM scores vary widely (z_k from -0.5 to 0.95, high σ_k). High variance encourages extended sampling ($K \geq 5$, approaching n), maximizing the chance of finding a high-quality response. This results in high diversity, capturing varied response quality. In AMC23, 25% of queries exhibited this behavior. A failure mode occurs if σ_k remains high due to RM noise, leading to excessive sampling (observed in 3% of cases).

• High-Patience Configurations: When configured with low c or high n (e.g., Example 5: “Outline three approaches to solving climate change”), BEACON extends sampling even after finding good responses ($z_k \approx 0.85 - 0.92$). A lower c reduces the effective cost threshold (c/σ_k), encouraging exploration for

1665 potentially better or more diverse solutions. framework.
1666 This leads to late stopping ($K \geq 6$) and high
1667 diversity. In experiments with $c = 0.1$, 50%
1668 of queries extended to $K \geq 8$, enhancing so-
1669 lution variety. A failure mode is unnecessary
1670 computation if high-quality responses are al-
1671 ready sufficient (observed in 4% of cases).

1672 To quantify failure modes, we analyzed 100
1673 MATH500 queries and found that premature stop-
1674 ping (due to RM miscalibration) occurred in 2–3%
1675 of cases, while excessive sampling (due to persis-
1676 tent high σ_k) occurred in 3–5% of cases. These are
1677 mitigated by the robust updating formula, which
1678 filters outliers to stabilize σ_k . BEACON thus dy-
1679 namically adjusts exploration based on reward con-
1680 sistency (σ_k), response quality (z_k, μ_k), and budget
1681 ($n - k$), aligning with the trade-offs specified by
1682 c and n . This ensures efficient high-reward sam-
1683 ple selection across query difficulties, with failure
1684 modes addressed through robust design.

1685 F Reproducibility Statement

1686 To facilitate reproducibility of our work, we have
1687 made significant efforts to document all implemen-
1688 tation details and experimental procedures. The
1689 complete source code for BEACON is available
1690 through a repository referenced in [anonymous](#)
1691 [GitHub repository](#), including implementations of
1692 all baseline methods, reward model integrations,
1693 and evaluation protocols. Our theoretical contribu-
1694 tions include complete proofs in Appendix D.7 and
1695 detailed derivations of the Universal Index Policy
1696 with explicit formulations for the h-index computa-
1697 tion (Appendix D.5). All experimental configura-
1698 tions are thoroughly documented in Appendix A.1,
1699 specifying exact model versions, API endpoints,
1700 hyperparameter settings, and evaluation protocols
1701 for both reasoning and alignment benchmarks. We
1702 provide comprehensive hyperparameter selection
1703 guidelines (Appendix B). The paper includes ex-
1704 plicit algorithmic descriptions (Algorithm 1), suffi-
1705 cient statistics formulations (Appendix D.3), and
1706 complete experimental results with statistical sig-
1707 nificance analysis (Appendix E.1). All datasets
1708 used are publicly available, and our evaluation pro-
1709 cedures follow standard protocols from established
1710 benchmarks (MATH, AIME, AMC, AlpacaEval
2.0). Additionally, we provide extensions to dis-
1711 crete reward scenarios (Appendix D.6) and prac-
1712 tical implementation guidance for batch-parallel
1713 deployments to ensure broad applicability of our